Geological Society of America Bulletin

High-precision U-Pb calibration of Carboniferous glaciation and climate history, Paganzo Group, NW Argentina

E.L. Gulbranson, I.P. Montañez, M.D. Schmitz, C.O. Limarino, J.L. Isbell, S.A. Marenssi and J.L. Crowley

Geological Society of America Bulletin 2010;122;1480-1498
doi: 10.1130/B30025.1

Notes

High-precision U-Pb calibration of Carboniferous glaciation and climate history, Paganzo Group, NW Argentina

E.L. Gulbranson[1,†], I.P. Montañez[1], M.D. Schmitz[2], C.O. Limarino[3,4], J.L. Isbell[5], S.A. Marenssi[3,4,6], and J.L. Crowley[2]

[1]*Department of Geology, University of California, One Shields Avenue, Davis, California 95616, USA*
[2]*Department of Geosciences, Boise State University, Isotope Geology Laboratory, Boise, Idaho 83725, USA*
[3]*Department of Geology, University of Buenos Aires, Cuidad Universitaria, Pabellón II, 1428, Buenos Aires, Argentina*
[4]*Consejo Nacional de Investigaciones Cientificas y Técnicas (CONICET), Sarmiento 440, Buenos Aires, Argentina*
[5]*Department of Geology, University of Wisconsin, Milwaukee, Wisconsin 53211, USA*
[6]*Instituto Antártico Argentino, Cerrito 1248, C1010AAZ Buenos Aires, Argentina*

ABSTRACT

The duration and geographic extent of Carboniferous glacial events in southern Gondwana remain poorly constrained despite recent evidence for a more dynamic glacial history than previously considered. We report 10 high-precision (2σ ± <0.1%) U-Pb ages for the Permian-Carboniferous Paganzo Group, NW Argentina, that redefine the chronostratigraphy of the late Paleozoic Paganzo and Río Blanco Basins, and significantly refine the timing of glacial events and climate shifts in the western region of southern Gondwana. Radiometric calibration of the Paganzo Group indicates three pulses of Carboniferous glaciation in the mid-Visean, the late Serpukhovian to earliest Bashkirian, and between the latest Bashkirian to early Moscovian.

An abrupt shift in depositional style from high-sinuosity single-storied fluvial deposits and clay-rich paleosols to low-sinuosity multistoried feldspathic fluvial deposits intercalated with eolianites and calcic paleosols is constrained to the latest Moscovian and earliest Kasimovian. These constraints indicate a relatively abrupt climate shift from humid-subhumid to nonseasonal semiarid regional climate conditions that occurred significantly earlier than previously inferred (Early Permian). This period of high-latitude aridity was contemporaneous with a shift to dryland depositional environments and a major vegetation regime shift documented throughout the Pangean paleotropics in the Pennsylvanian.

INTRODUCTION

As the longest-lived and most geographically extensive ice age of the Phanerozoic, the late Paleozoic ice age (LPIA) is the best-understood pre-Quaternary glaciation (Veevers and Powell, 1987; Crowley et al., 1989; Frakes et al., 1992; Gastaldo et al., 1996). Recent studies of near-field (proximal to ice-contact settings) glacigenic deposits (Isbell et al., 2008a, 2008b; Fielding et al., 2008a, 2008b) and paleotropical far-field successions (Rygel et al., 2008; Heckel, 2008; Bishop et al., 2009) reveal a more dynamic glaciation history than previously inferred from paleotropical stratigraphic archives (Heckel, 1994, 2002, and references therein), possibly involving an asynchronous series of alpine and continental glaciations separated by periods of minimal ice. Despite recent advances in our understanding of the late Paleozoic ice age, the timing, duration, style, and extent of discrete glaciations remain enigmatic, and thus hamper attempts to refine climate–sea level–glaciation linkages. This reflects in large part the lack of robust chronologies for constraining and correlating stratigraphic successions and their proxy records.

The Paganzo and Río Blanco Basins of northwest Argentina (Fig. 1) archive stratigraphic and sedimentologic evidence of glaciation interleaved with nonglaciated periods inferred from facies patterns and the stratigraphic architecture of paralic deposits (fluvial, deltaic, marine, lacustrine) and associated paleosols (López Gamundí, 1987; Limarino et al., 2006). To date, study of these Upper Paleozoic successions has been reconnaissance in nature, focusing on basic stratigraphy and paleontology (e.g., Taboada, 1985; Archangelsky et al., 1987; Andreis et al., 1987; Azcuy et al., 1987a, 1987b; González, 1981, 1990). Despite the importance of these strata to the advancement of near-field late Paleozoic ice age studies, only recently have studies in these basins begun to analyze the strata using modern glacial facies analysis or sequence stratigraphic techniques (e.g., Pazos, 2002b; López-Gamundí and Martinez, 2003; Marenssi et al., 2005; Limarino et al., 2006; Henry et al., 2008). Notably, these Gondwanan successions host an abundance of volcanogenic deposits, providing an opportunity to develop a high-resolution chronostratigraphic framework for these ice-proximal basins through U-Pb dating of zircons.

Here, we present the first high-precision U-Pb ages (2σ ± <0.1%) for volcanics from the Permian-Carboniferous Paganzo Group of northwestern Argentina. Our results confirm a proposed (Limarino et al., 2006; Caputo et al., 2008) mid-Visean age for the onset of glaciation in southwestern Gondwana and constrain a second pulse of Carboniferous glaciation (Marenssi et al., 2005; Césari and Gutiérrez, 2000; Limarino et al., 2006; Henry et al., 2008) to the Serpukhovian–early Bashkirian. A third, previously unrecognized interval of distal glacigenic deposits is constrained by U-Pb ages to the late Bashkirian–early Moscovian. These radiometrically calibrated glacigenic intervals coincide with two of four Carboniferous glaciations recently defined from the eastern Gondwana margin in eastern Australia (Jones and Fielding, 2004; Fielding et al., 2008a, 2008b), thus indicating near synchrony between short-lived glacial events on the western and eastern margins of Gondwana. In addition, U-Pb constraints on the duration of the Paganzo Group indicate that the pronounced shift in depositional style of fluvio-deltaic facies and the introduction of eolian deposits, long believed to record the

[†]E-mail: gulbranson@geology.ucdavis.edu

GSA Bulletin; September/October 2010; v. 122; no. 9/10; p. 1480–1498; doi: 10.1130/B30025.1; 9 figures; 3 tables; Data Repository item 2010053.

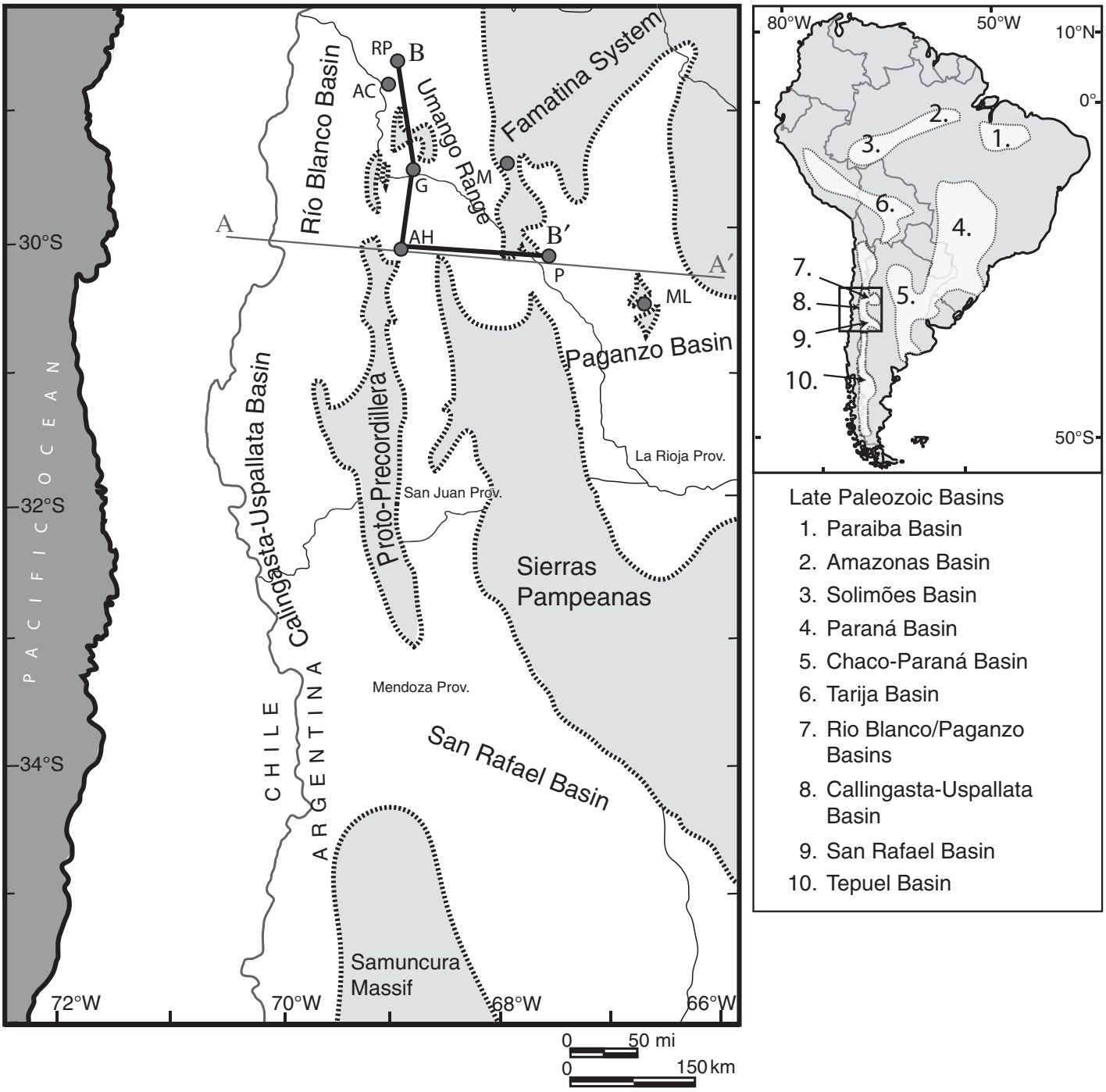

Figure 1. Map of the study area: darker areas denote paleotopographic highs (Limarino et al., 2006). Filled circles show the locations of measured sections used in the study and presented in this paper (AH, RP, and G). Cross-section line A–A′ shows the location for the cross-section diagram in Figure 2; B–B′ shows the location of the cross-section of Figure 8. The smaller map of South America highlights the location of late Paleozoic basins; numbers correspond to basin names in the box below. AH—Agua Hedionda anticline section (Huaco area), G—Cerro Guandacol section, AC—Agua de Carlos section, RP—Río del Peñon section, M—Cuesta de Miranda section, P—Paganzo section, ML—Malanzán-Olta section.

long-term Permian aridification of Pangea, rather records a relatively abrupt late Moscovian to earliest Kasimovian climate change coincident with a major drying event revealed by paleotropical Euramerican successions (Tabor and Montañez, 2005; Montañez et al., 2008; Bishop et al., 2010).

TECTONIC AND STRATIGRAPHIC SETTING

The Paganzo and Río Blanco Basins are situated proximal to the Andean Precordillera of northwestern Argentina (Fig. 1), which served as the active southwestern (Panthalassan) margin of Gondwana during the early Paleozoic (Fig. 2). Paleogeographic reconstructions indicate that the study area remained between 40°S and 50°S during the Visean to Asselian time interval (Scotese and Barrett, 1990; Torsvik and Cocks, 2004; Blakey, 2008), followed by northward migration of South America throughout the Permian (Scotese et al., 1999; Van der Voo and Torsvik, 2001). Several allochthonous terranes were accreted to this margin during the early Paleozoic (Ramos et al., 1984; Keller, 1999; Pankhurst et al., 2000), forming multiple recognizable tectonic provinces in northwestern Argentina, including the Sierras Pampeanas and the Cuyania terrane (Ramos, 2004). Thrusting of the Cuyania terrane during the mid-Paleozoic Chañic orogeny formed the proto–Precordillera and back-arc basins along the active margin (Limarino et al., 2006; Henry et al., 2008). During the late Devonian Río Blanco tectonic event, accretion of the disputed Chilenia terrane further augmented basin development initiated during the Chañic orogeny (López Gamundí, 1997; Limarino et al., 2006; Henry et al., 2008). The Río Blanco back-arc basin and Paganzo foreland basins subsequently underwent extensional collapse during the Late Permian (Limarino and Spalletti, 1986), and subsidence rates presumably slowed, allowing aggradational basin filling (Limarino et al., 2006).

The Río Blanco Basin, which developed during the Chañic orogeny, was situated outboard (west) of the proto–Precordillera as a foreland basin (Scalabrini Ortiz, 1973). Initial mixed terrestrial and marine sedimentation (Angualasto Group) culminated with glacial diamictites of probable Visean age (Limarino et al., 2006). These deposits were later deformed during the Río Blanco tectonic event, which modified the foreland basin to a back-arc basin (Fig. 2). The overlying Paganzo Group sediments in the Río Blanco Basin contain a basal diamictite of glacigenic origin (Gulbranson et al., 2008), which in turn is overlain by fluvio-deltaic sediments that pass upward to deep-marine to siliciclastic shoreface facies.

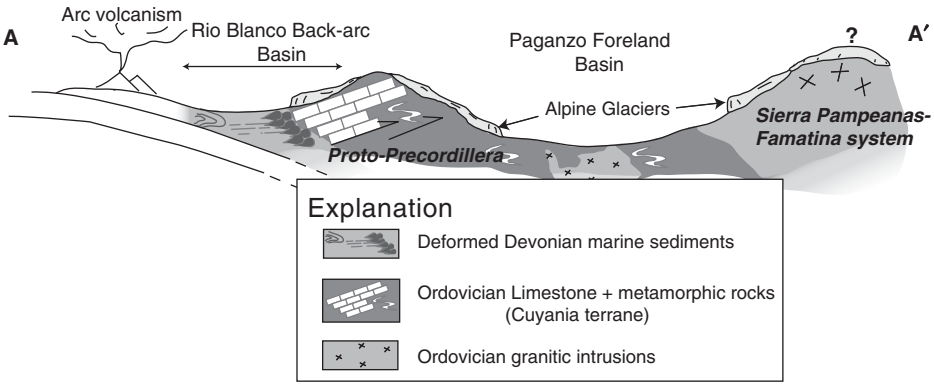

Figure 2. Geologic cross-section from A–A′ (Fig. 1). Major geologic components are shown from west to east: deformed Devonian marine sediments and pillow basalts, the Cuyania terrane, composed of Cambrian to Ordovician marine carbonates and early Paleozoic metamorphic rocks, and Ordovician intrusive rocks of the Sierra Pampeanas–Famatina system.

The Paganzo Basin developed in the mid-Carboniferous as an eastward-facing foreland basin east of the proto–Precordillera hinterland (Limarino et al., 2006). Remnants of the Chañic orogeny were present in the Paganzo Basin as paleotopographic highs of the Famatina-Pampeanas system, and localized uplifts (Umango Range, Figs. 1 and 2; Limarino et al., 2006). The accretion of Chilenia during the Río Blanco tectonic phase, although controversial, is recorded in the Paganzo Basin as an erosional unconformity separating Pennsylvanian sedimentary rocks of the Paganzo Group from Ordovician and Precambrian rocks of the Cuyania terrane (Fig. 3). Initial basin-filling sediments in the proto–Precordillera region and in areas proximal to paleotopographic highs are diamictites of glacial origin (López Gamundí, 1987; López Gamundí and Breitkreuz, 1997; Pazos, 2002b; Marenssi et al., 2005). Carboniferous shallow-marine and deltaic deposits overlie the glacigenic strata, and are in turn overlain by presumed Permian-age eolian, braided stream, avulsion, and playa-lake deposits basinwide.

Permian-Carboniferous sedimentary deposits in the Río Blanco and Paganzo Basins belong to the Paganzo Group of northwestern Argentina, which consists of several formal rock units (Fig. 4). In this paper, we divide the Paganzo Group into three stratigraphic intervals (SI) defined on the basis of the established stratigraphy. These stratigraphic intervals incorporate existing lithostratigraphic units (e.g., Patquia Formation) and are placed into a temporal framework defined by radiometric calibration (Fig. 4). SI-1 includes Serpukhovian to early Bashkirian strata (Guandacol Formation and equivalent units), SI-2 includes Bashkirian to early Moscovian strata (Tupe Formation and equivalent units), and SI-3 includes Moscovian through Permian strata (Patquia Formation and equivalent units). Initial basin fill (SI-1) of the Paganzo Group began with deposition of diamictites or dropstone-bearing mudstones, but transitioned rapidly to shallow-marine or deltaic deposition with a decrease in dropstone-bearing sediments. An erosional surface marks the contact between SI-1 and SI-2 in the Río Blanco Basin, but this surface is conformable to the east in Paganzo Basin (Limarino et al., 2006). SI-2 incorporates aggradational and progradational deposits of the Río Blanco and Paganzo Basins and is dominated by fluvio-deltaic facies, coals, and black shales. SI-3 is the final phase of basin fill and is marked by stratigraphic onlap onto paleotopographic highs (Limarino and Spalletti, 1986) and a change from paralic-dominated to terrestrial-dominated sedimentation. The three stratigraphic units record a three-phase basin filling of the Río Blanco and Paganzo Basins, and define second-order sequences in the Paganzo Group (Limarino et al., 2006).

METHODOLOGY

Volcanogenic deposits were collected from the Paganzo Group in the western Paganzo and Río Blanco Basins, NW Argentina (Fig. 1). Samples were obtained within a framework defined by three stratigraphic sections from the Río Blanco Basin, and five sections from the Paganzo Basin, which were measured and described at the decimeter scale. Samples include ignimbrites of various grain sizes, ashes, and tonsteins (i.e., altered ashes within coal seams). Sample collection focused on the basal portion of the ignimbrite or ash to account for the settling of zircon during deposition.

Zircons were separated by standard methods of crushing, magnetic separation, and heavy

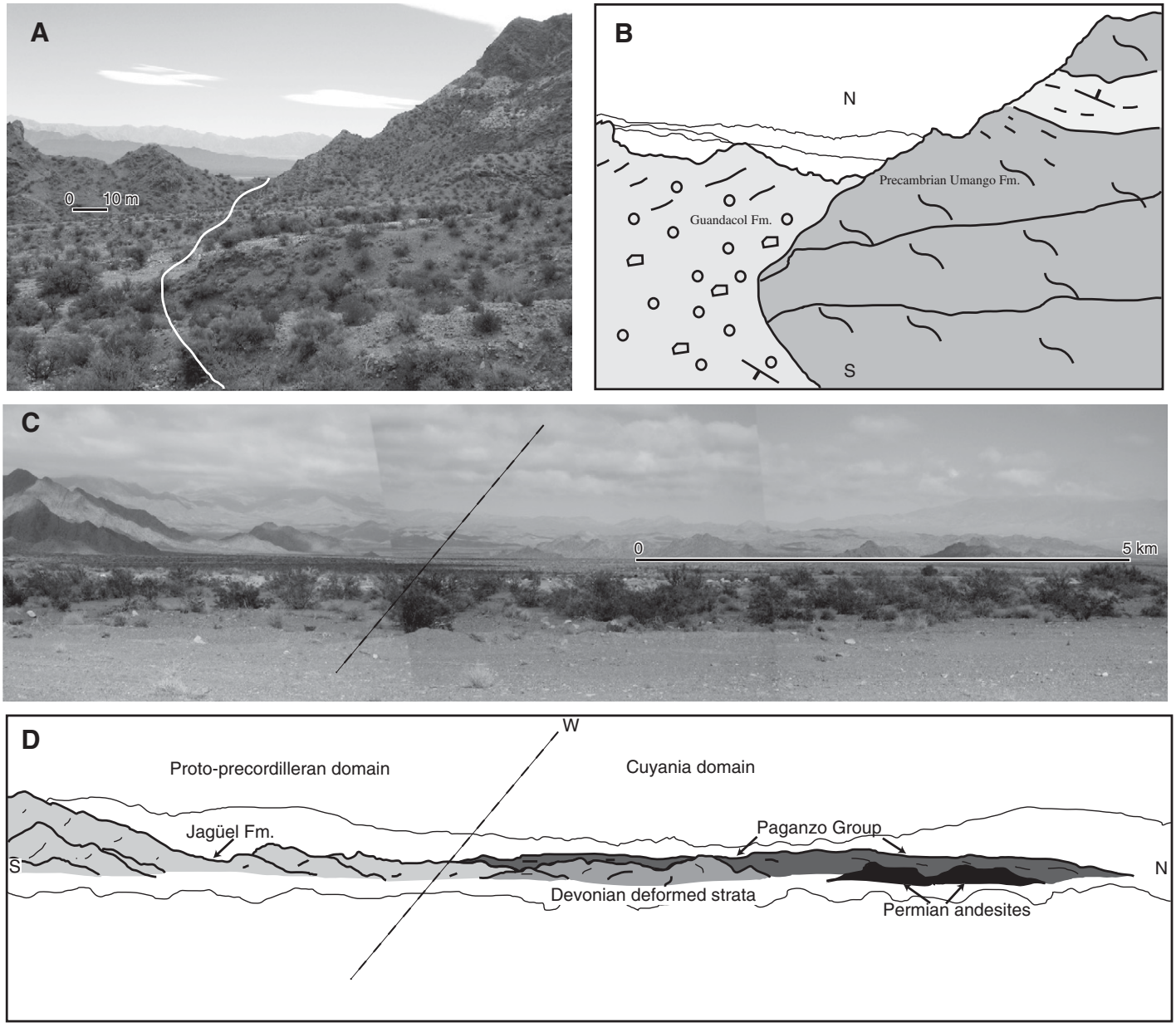

Figure 3. (A) Photograph and (B) diagram of the contact between the basal diamictite of SI-1 (Guandacol Formation) and early Paleozoic metamorphic rocks (Umango Formation). Large clasts in the diamictite are predominantly metamorphic lithologies (schist, quartzite, etc.); the light tan band in (A) and highlighted in (B) is a zone of quartzite-rich material. (C–D) Stratigraphic relationship between the Jagüel Formation (Cortaderas Formation) and the Paganzo Group near the AC locality (Fig. 1). The basal diamictites of SI-1 (lower Río del Peñon Formation) are seen as unconformably overlying both the Jagüel Formation (Cortaderas Formation) and the Punta del Aqua Formation (not shown here, but it is exposed to the north). In turn, the Jagüel Formation rests unconformably against deformed Devonian strata seen in the foreground. The dashed line in both the photomosaic and diagram represents the general boundary between the proto-Precordilleran domain and Cuyania domain, which comprise the Cuyania terrane (C.O. Limarino, 2008, personal commun.).

liquid separation. Handpicked zircons were subjected to a modified version of the chemical abrasion method of Mattinson (2005), reflecting a preference to prepare and analyze carefully selected single crystals or crystal fragments. Zircon separates were placed in a muffle furnace at 900 °C for 60 h in quartz beakers for annealing. Single crystals were transferred to 3 mL Teflon perfluoroalkoxy (PFA) beakers, rinsed twice with 3.5 *M* HNO_3, and loaded into 300 µL Teflon PFA microcapsules. Fifteen microcapsules were placed in a large-capacity Parr vessel, and the crystals were partially dissolved in 120 µL of 29 *M* HF with a trace of 3.5 *M* HNO_3 for 10–12 h at 180 °C. The contents of each microcapsule were returned to 3 mL Teflon PFA beakers, the HF was removed, and the residual grains were rinsed in ultrapure H_2O, immersed in 3.5 *M* HNO_3, ultrasonically cleaned for an hour, and fluxed on a hotplate at 80 °C for 1 h. The HNO_3 was removed, and the grains were again

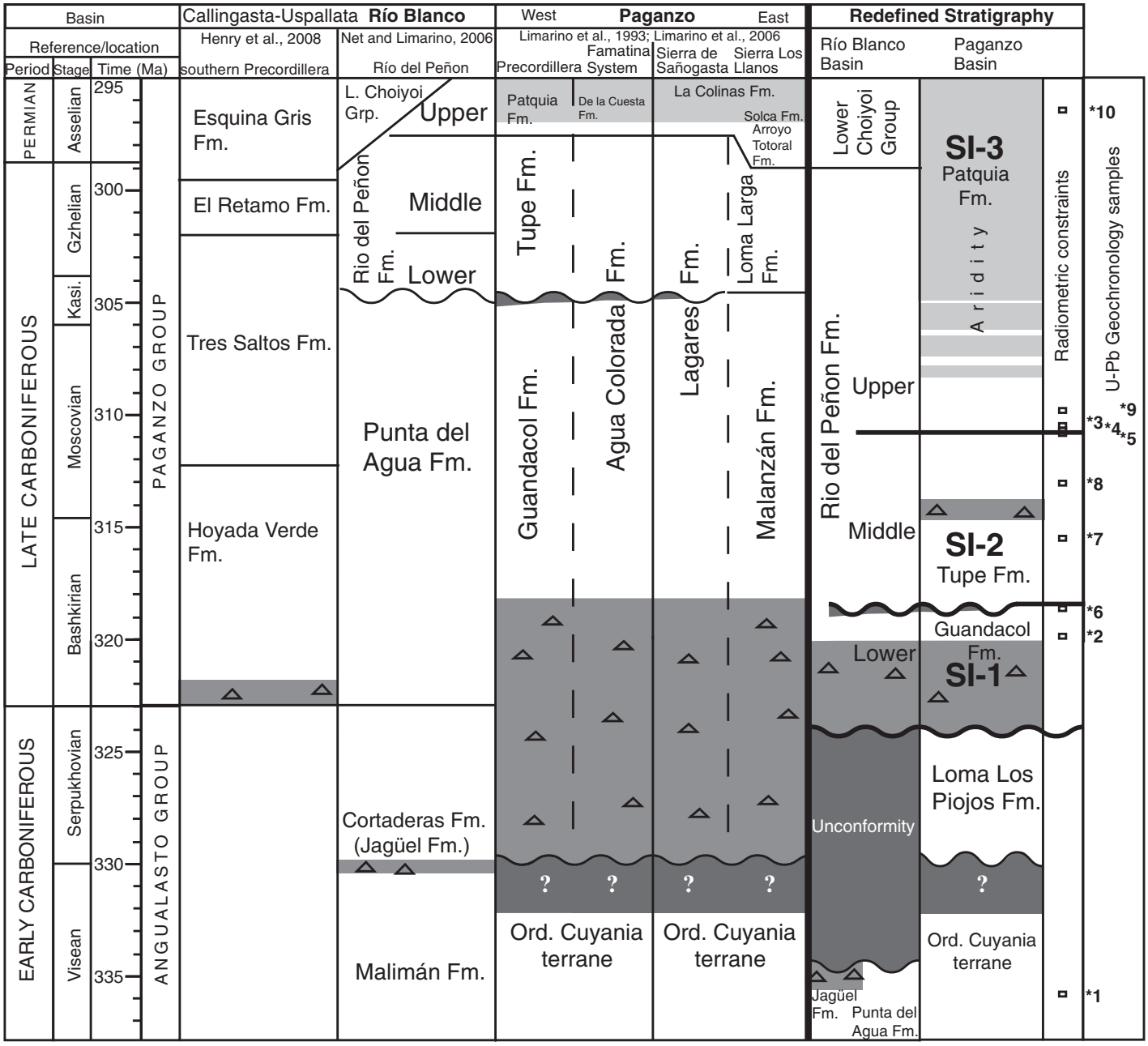

Figure 4. Chronostratigraphy of the Paganzo and Angualasto Groups from the modern Andean Precordilleran region to the Sierra Pampeanas. Columns to the left of the vertical bold line document the established stratigraphy for the Paganzo Group throughout the Rio Blanco and Paganzo Basins; the rightmost column represents the redefined stratigraphy presented here and includes the recently described Loma de los Piojos Formation (Balseiro et al., 2009). Formation names and age ranges are listed against the Carboniferous time scale (Davydov et al., in press). Dark-gray shading denotes unconformities; question mark indicates an unknown temporal extent of an unconformity. Medium-gray shading with triangle symbols indicates the temporal extent of glacigenic deposits. Light-gray shading denotes sedimentary evidence of aridity (e.g., eolianites, playa-lake deposits). Wavy lines indicate erosional contacts. SI-1, SI-2, and SI-3 are referred to in the text. Radiometric constraints are shown in the rightmost column and referenced to sample number (e.g., *2): *1—07VD-36, *2—07VD-35, *3—RPTIgn-1, *4—GPIgn-1, *5—07VD-26, *6—07VD-13, *7—07VD-5, *8—07VD-6, *9—07VD-8, *10—PPAsh-1.

rinsed in ultrapure H_2O or 3.5 *M* HNO_3 before being reloaded into the same 300 µL Teflon PFA microcapsules (rinsed and fluxed in 6 *M* HCl during crystal sonication and washing) and spiked with the EARTHTIME (Condon, 2005; Parrish et al., 2006) mixed ^{205}Pb-^{233}U-^{235}U tracer solution (ET535). These chemically abraded grains were dissolved in Parr vessels in 120 µL of 29 *M* HF with a trace of 3.5 *M* HNO_3 at 220 °C for 48 h, dried to fluorides, and then redissolved in 6 *M* HCl at 180 °C overnight. U and Pb were separated from the zircon matrix using an HCl-based anion-exchange chromatographic procedure (Krogh, 1973), eluted together, and dried with 2 µL of 0.05 *N* H_3PO_4.

Pb and U were loaded on a single outgassed Re filament in 2 µL of a silica-gel/phosphoric acid mixture (Gerstenberger and Haase, 1997). U and Pb isotopic measurements were made on an Isoprobe-T multicollector thermal ionization mass spectrometer (TIMS) equipped with an ion-counting Daly detector at the Boise State University Isotope Geology Laboratory. Pb isotopes were measured by peak-jumping all isotopes on the Daly detector for 100–150 cycles, and corrected for 0.22 ± 0.04%/a.m.u. mass fractionation. Transitory isobaric interferences due to high-molecular-weight organics, particularly on ^{204}Pb and ^{207}Pb, disappeared within ~30 cycles, while ionization efficiency averaged 10^4 cps/pg. Linearity (to $\geq 1.4 \times 10^6$ cps) and the associated deadtime correction of the Daly detector were monitored by repeated analyses of NBS982, and have been constant since installation (2006). Uranium was analyzed as UO_2^+ ions in static Faraday mode on 10^{11} ohm resistors for 150–200 cycles, and corrected for isobaric interference of $^{233}U^{18}O^{16}O$ on $^{235}U^{16}O^{16}O$ with an $^{18}O/^{16}O$ of 0.00205. Ionization efficiency averaged 20 mV/ng U. U mass fractionation was corrected using the known $^{233}U/^{235}U$ ratio of the ET535 tracer solution.

U-Pb dates and uncertainties for each analysis were calculated using the algorithms of Schmitz and Schoene (2007) and a $^{235}U/^{205}Pb$ ratio for ET535 of 100.18 ± 0.05. The $^{206}Pb/^{238}U$ ratios and dates were corrected for initial ^{230}Th disequilibrium using a Th/U[magma] of 3 (Crowley et al., 2007), resulting in a systematic increase in the $^{206}Pb/^{238}U$ dates of ~90 k.y. Common Pb in analyses was attributed to laboratory blank and subtracted based on the measured laboratory Pb isotopic composition and associated uncertainty. U blanks were less than 0.1 pg, and correction was insignificant. Over the course of the experiment, isotopic analyses of the TEMORA zircon standard yielded a weighted mean $^{206}Pb/^{238}U$ age of 417.43 ± 0.06 (n = 11, mean square of weighted deviates [MSWD] = 0.8). The quoted age error includes analytical uncertainties based on counting statistics, spike subtraction, and common Pb correction, and is appropriate in comparisons with other $^{206}Pb/^{238}U$ ages obtained with the EARTHTIME spike, or those spikes cross-calibrated with the EARTHTIME gravimetic standards. If used in comparison with ages derived from other U-Pb methods or decay schemes (e.g., Ar/Ar, ^{187}Re-^{187}Os), then the uncertainty in the spike U/Pb ratio and the ^{238}U decay constant can be added in quadrature, respectively. Quoted errors for individual analyses are of the form ±X [Y/Z] (sensu Bowring et al., 2007) where X is analytical uncertainty, Y is the combined analytical and tracer uncertainty, and Z is the combined analytical, tracer, and ^{238}U decay constant uncertainty.

In total, 72 single zircon grains from 10 samples were analyzed. Eight grains were grossly discordant, reflecting the presence of ancient inherited cores. All data sets yielded majority clusters of concordant (considering decay constant errors) and equivalent dates that we interpret as the igneous crystallization ages of the zircons, and that approximate the eruption and deposition ages of the volcanic horizons (Reid and Coath, 2000; Crowley et al., 2007). We discard from age calculations the dates resolvable from the majority cluster at the 95% confidence interval (CI), interpreted as antecrysts (Miller et al., 2007) inherited from earlier episode(s) of magmatism or from juvenile basement to the magmatic system. The rarity of younger outliers in each data set attests to the efficacy of the chemical abrasion method for removing domains affected by Pb loss. The mean square of the weighted deviates (MSWD, York, 1967, 1969) was calculated for the weighted mean $^{206}Pb/^{238}U$ ages of the majority clusters. Utilizing the statistical distribution of MSWD (Wendt and Carl, 1991), for n – 1 degrees of freedom, we calculated the acceptable degree of data scatter attributable to analytical errors; all weighted mean ages pass this confidence test at the 95% CI.

U-Pb RESULTS AND STRATIGRAPHIC CONTEXT

Volcanic zircon populations were successfully separated from altered volcanic ashes (bentonites), tuffs, medium- to coarse-grained ignimbrites (rarely exhibiting cross lamination) and andesites from the Paganzo Group in both study basins, as well as one sample from the top of the underlying Punta del Agua Formation, which, according to the new ages presented in this paper, would correlate with the upper part of the Angualasto Group (Fig. 4). Fifty samples were collected for zircon extraction and U-Pb geochronology. Of these, 16 yielded zircons suitable for analysis, and 10 samples were used for U-Pb age determination. The analytical data are located in the GSA Data Repository (Table S1[1]), and the resulting ages and statistical parameters are summarized in Table 1. Bentonite-rich clays dominate the lower portion of the Paganzo Group (SI-1 and SI-2) and occur either as clay-rich layers in delta-plain facies, or as silicate-rich horizons in Histosols, where these clays are dominated by kaolinite (Net et al., 2002). Ignimbrites occur in SI-3, typically in the basal terrestrial floodplain sediments and

[1]GSA Data Repository item 2010053, U-Th-Pb isotopic data and isotopic ages for all zircons used in this study, organized by sample name as it appears in the text, is available at http://www.geosociety.org/pubs/ft2010.htm or by request to editing@geosociety.org.

TABLE 1. U-PB AGE RESULTS

Sample	Formation (SI)	Rock type	Number of analyses*	$^{206}Pb/^{238}U$ age (Ma)	±X†	±Y/Z§	MSWD#
O7VD-36	Punta del Aqua	Andesite	12, 7	335.99	0.06	0.18/0.39	1.3
07VD-35	Lower Río del Peñon	Tuff	7, 6	319.57	0.09	0.18/0.38	1.0
RPTIgn-1	Middle Río del Peñon	Ignimbrite	7, 5	310.63	0.07	0.17/0.37	2.0
GPIgn-1	Patquia	Ignimbrite	8, 5	310.93	0.08	0.17/0.37	1.2
07VD-26	Patquia	Ignimbrite	6, 5	309.89	0.08	0.17/0.37	1.0
07VD-13	Guandacol	Ash	7, 5	318.79	0.10	0.19/0.38	1.17
07VD-5	Tupe	Tonstein	5, 5	315.46	0.07	0.17/0.37	0.8
07VD-6	Tupe	Tonstein	5, 4	312.82	0.11	0.19/0.38	2.1
07VD-8	Patquia	Ash	9, 4	310.71	0.11	0.19/0.38	1.1
PPAsh-1	Las Colinas	Tuff	6, 5	296.09	0.08	0.17/0.35	0.67

Note: Ages were calculated using concordant zircons; excluded grains are identified in the text and the GSA Data Repository (see text footnote 1).

*The number preceding comma reflects total grains analyzed, and the number after comma reflects grains used in age calculation.

†X represents analytical uncertainty.

§Y represents analytical and tracer uncertainties, and Z represents analytical, tracer, and ^{238}U decay constant uncertainties.

#Mean square of weighted deviates: an MSWD of 1 is ideal (Wendt and Carl, 1991), MSWD << 1 may indicate overestimated analytical uncertainty, and MSWD > 2 reflects scatter outside of the 95% confidence interval, indicating geologic uncertainty.

fluvial deposits. Ignimbrites are medium- to coarse-grained mixtures of lithic fragments, devitrified glass, phenocrystic biotite, and secondary chlorite/epidote. Near the upper contact of SI-3, the volcanic deposits occur as finer-grained, glassy, porous, and low-bulk-density ashes, primarily from within low-sinuosity fluvial, playa-lake, and eolian deposits.

Río Blanco Basin, Río del Peñon Section

Three samples from the Río del Peñon locality ("RP"; Fig. 1) contained zircon populations suitable for U-Pb geochronology. The stratigraphically lowest sample was collected from an andesite of the Punta del Agua Formation in contact with diamictites of SI-1. Both the Punta del Aqua Formation and the diamictite-bearing Cortaderas Formation (Angualasto Group; Figs. 3B and 4) are in unconformable contact with SI-1. In light of the U-Pb ages presented here (Table 1) and the Visean-age flora extracted from the Cortaderas Formation (Fauqué et al., 1989; César and Limarino, 1992; Perez Loinaze, 2007), we propose that the Cortaderas Formation diamictites are time equivalent to the upper Punta del Agua Formation. Previously, the Punta del Agua Formation was considered Pennsylvanian to perhaps Early Permian in age (Fig. 4; Fauqué et al., 1999; Remesal et al., 2004).

Twelve transparent zircons exhibiting bipyramidal terminations, sharp crystal faces and edges, and minor inclusions of devitrified glass were analyzed from this andesite (07VD-36). Seven grains provide a concordant weighted mean $^{206}Pb/^{238}U$ age of 335.99 ± 0.06 [0.18/0.39] Ma (2σ, MSWD = 1.3). The high precision of isotope dilution–thermal ionization mass spectrometer (ID-TIMS) analyses elucidates three grains that are clearly older than the majority cluster (Fig. 5A), and these are interpreted to reflect inheritance. Two additional grains are younger than the majority cluster, probably due to Pb loss (Fig. 5A). This defines a maximum age for the basal diamictite of the Guandacol Formation (SI-1) and a minimum age for the stratigraphically oldest glacial deposit recorded in the Cortaderas Formation (Fig. 5A). A second sample (07VD-35) was collected from post-glacial deposits immediately overlying the SI-1 basal diamictites at Río del Peñon (Gulbranson et al., 2008). Six out of seven zircons analyzed from this sample (07VD-35) yield a concordant weighted mean $^{206}Pb/^{238}U$ age of 319.57 ± 0.09 [0.18/0.38] Ma (2σ, MSWD = 1.0, Fig. 5A), constraining the glacial event to the late Serpukhovian–earliest Bashkirian. One zircon from this sample is marginally older and is interpreted as an inherited zircon grain. Five out of seven zircons from sample RPTIgn (Fig. 5A), an ignimbrite collected from fluvio-deltaic deposits of the upper portion of SI-2, yield a concordant weighted mean $^{206}Pb/^{238}U$ age of 310.63 ± 0.07 [0.17/0.37] Ma (2σ, MSWD = 2.0). The two grains not used in the age calculation are clearly older and reflect inheritance.

Paganzo Basin, Cerro Guandacol Section

Two samples were chosen for U-Pb analysis from the Cerro Guandacol locality (Table 1), western Paganzo Basin ("G"; Figs. 1 and 5B). Eight zircon grains were analyzed from a homogeneous population of prismatic zircons collected from an ignimbrite (GPIgn-1) within fluvial-floodplain facies near the base of the SI-3. Five precise and concordant $^{206}Pb/^{238}U$ ages provide a weighted mean age of 310.93 ± 0.08 [0.17/0.37] Ma (2σ, MSWD = 1.2; Fig. 5B). Of the three grains not used in the age calculation, two are significantly older, indicating inheritance, and one is resolvably younger, reflecting Pb loss. Five out of six analyzed zircons from a second ignimbrite, 07VD-26 (Fig. 5B), ~65 m above the first ignimbrite, yield a concordant weighted mean $^{206}Pb/^{238}U$ age of 309.89 ± 0.08 [0.17/0.37] Ma (2σ, MSWD = 1.0). One zircon is Neoproterozoic in age, which may reflect xenocrystic zircon incorporated, via anatexis, into the magmatic system that generated this tuff.

Paganzo Basin, Huaco Section

Four samples of altered volcanic ash collected from floodplain, peat bog, and delta plain siliciclastic facies at the Aqua Hedionda anticline section near Huaco ("AH"; Figs. 1 and 6) contained zircons suitable for U-Pb analysis. Seven zircons were analyzed from sample 07VD-13, collected below the contact of SI-1 (Guandacol Formation) and SI-2 (Tupe Formation). Five of these zircons yield a concordant weighted mean $^{206}Pb/^{238}U$ age of 318.79 ± 0.10 [0.19/0.38] Ma (2σ, MSWD = 1.17; Fig. 5C). Two zircons from this sample yield older ages, interpreted as inherited zircon grains. Sample 07VD-5, collected from a tonstein within progradational fluvial deposits of SI-2 (Tupe Formation), yields a group of five zircons with a weighted mean $^{206}Pb/^{238}U$ age of 315.46 ± 0.07 [0.17/0.37] Ma (2σ, MSWD = 0.8; Fig. 5C). Four of five zircons from sample 07VD-6, collected from a tonstein within an interval of intercalated paleosols and shallow-marine sandstones in upper SI-2 strata, yield a concordant weighted mean $^{206}Pb/^{238}U$ age of 312.82 ± 0.11 [0.19/0.38] Ma (2σ, MSWD = 2.1). One grain from this sample is resolvably younger, perhaps as a result of Pb loss, and is not used in the age calculation (Fig. 5C). Four out of nine zircons from the stratigraphically highest sample, 07VD-8 (Fig. 5C), collected from an ash deposit within anastomosing fluvial facies in SI-3 (Patquia Formation), yield a weighted mean $^{206}Pb/^{238}U$ age of 310.71 ± 0.11 [0.19/0.38] Ma (2σ, MSWD = 1.1). Four zircons are discordant and are significantly older than the four concordant analyses (see GSA Data Repository [see footnote 1]). One additional zircon from this sample yields a concordant Devonian age (406 Ma), suggesting that xenocrystic zircon forms a portion of this zircon population. This age is significantly younger than ages reported for inherited zircons from S-type granites (Pankhurst et al., 2000) of the Famatinian Belt (Fig. 1A). Alternatively, the disparity in ages may indicate that depositional reworking was important in forming this zircon population.

Paganzo Basin, Paganzo Section

One sample was selected for U-Pb analysis from the Paganzo locality (Table 1), central Paganzo Basin ("P"; Figs. 1 and 6). Five out of six zircon grains were analyzed from a population of prismatic zircons collected from a welded-tuff (PPAsh-1) in the upper part of eolian strata (upper portion of SI-3, Las Colinas Formation). Concordant U-Pb ages provide a weighted mean $^{206}Pb/^{238}U$ age of 296.09 ± 0.08 [0.17/0.35] Ma (2σ, MSWD = 0.67) for this sample (Fig. 5D). One grain is clearly older and concordant, indicating inheritance.

RADIOMETRIC CALIBRATION OF THE PAGANZO GROUP STRATIGRAPHY

The following sections synthesize the existing stratigraphic relationships established by previous studies of the Paganzo Group (Figs. 4 and 6) and discuss the new U-Pb constraints (Table 1) on the timing of glacial events and of major climate shifts recorded by Paganzo Group sediments in northwestern Argentina. We reference our new radiometric constraints to a global Carboniferous chronostratigraphic time scale (Table 2) recently calibrated with over 25 high-precision ID-TIMS U-Pb zircon ages (Davydov et al., 2010).

Stratigraphic Interval-1 and Equivalent Units

SI-1 includes the mid-Carboniferous Guandacol Formation, Lower Río del Peñon Formation, and equivalent units (Fig. 4), and is present throughout the modern Andean Precordilleran region and to the east toward the Sierras Pampeanas (López-Gamundí, 1987, 1997). An earlier interval of glaciation is recorded in

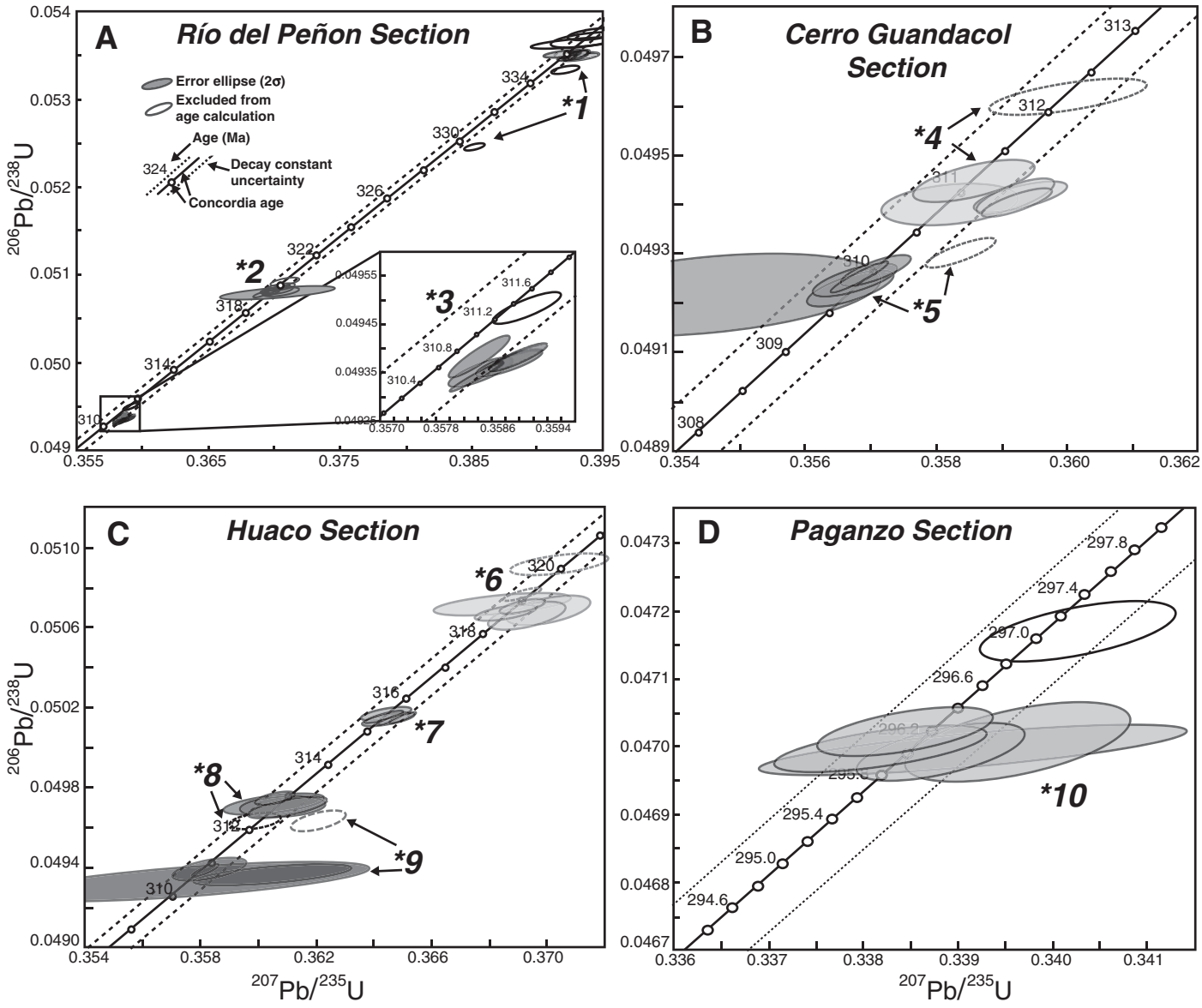

Figure 5. (A) Concordia diagram for samples collected at the Río del Peñon locality. Zircons are represented as error ellipses; shaded ellipses were used in the age calculation; and dashed and unfilled ellipses were excluded from age calculation (see text). (B) Concordia diagram of samples collected from the Cerro Guandacol locality. (C) Concordia diagram of samples collected at the Huaco locality. (D) Concordia diagram of samples collected from the Paganzo locality. Samples are referenced to the following list: *1—07VD-36, *2—07VD-35, *3—RPTIgn-1, *4—GPIgn-1, *5—07VD-26, *6—07VD-13, *7—07VD-5, *8—07VD-6, *9—07VD-8, *10—PPAsh-1.

diamictites of the Mississippian Cortaderas Formation, which is discussed following the description of SI-1 diamictites. Glacigenic sediments have been recognized in this stratigraphic unit since the early twentieth century (Bodenbender, 1911), and detailed descriptions and interpretations have been published in the last two decades (López-Gamundí, 1994; Pazos, 2002b; Marenssi et al., 2005). The basal glacigenic units of SI-1 overlie Mississippian andesites in the Río Blanco Basin and Ordovician and/or Precambrian rocks in the Paganzo Basin (Marenssi et al., 2005; Limarino et al., 2006). These sediments are laterally discontinuous at the basin scale and occur in paleovalleys and paleotopographic depressions on the underlying unconformity throughout the modern Andean Precordilleran region (Dykstra et al., 2006; Limarino et al., 2006; Kneller et al., 2004; Henry et al., 2008). Overlying the diamictites of SI-1, there are laminated siltstones and sandstones (Fig. 6) that are interpreted as prograding deltas during a postglacial transgression (Limarino et al., 2002; Pazos, 2002b; Limarino and Spalletti, 2006). Sedimentary facies corresponding to the postglacial transgression occur throughout the Paganzo and Río Blanco Basins and comprise the transgressive and highstand systems tract of the first depositional sequence of the Paganzo Group (Pazos, 2002b; Net and Limarino, 2006; Desjardins et al., 2009).

On the basis of observations made in the field and stratigraphic correlations between measured sections, we present the description of glacigenic sediments followed by a facies interpretation of glacigenic strata in SI-1. At the contact

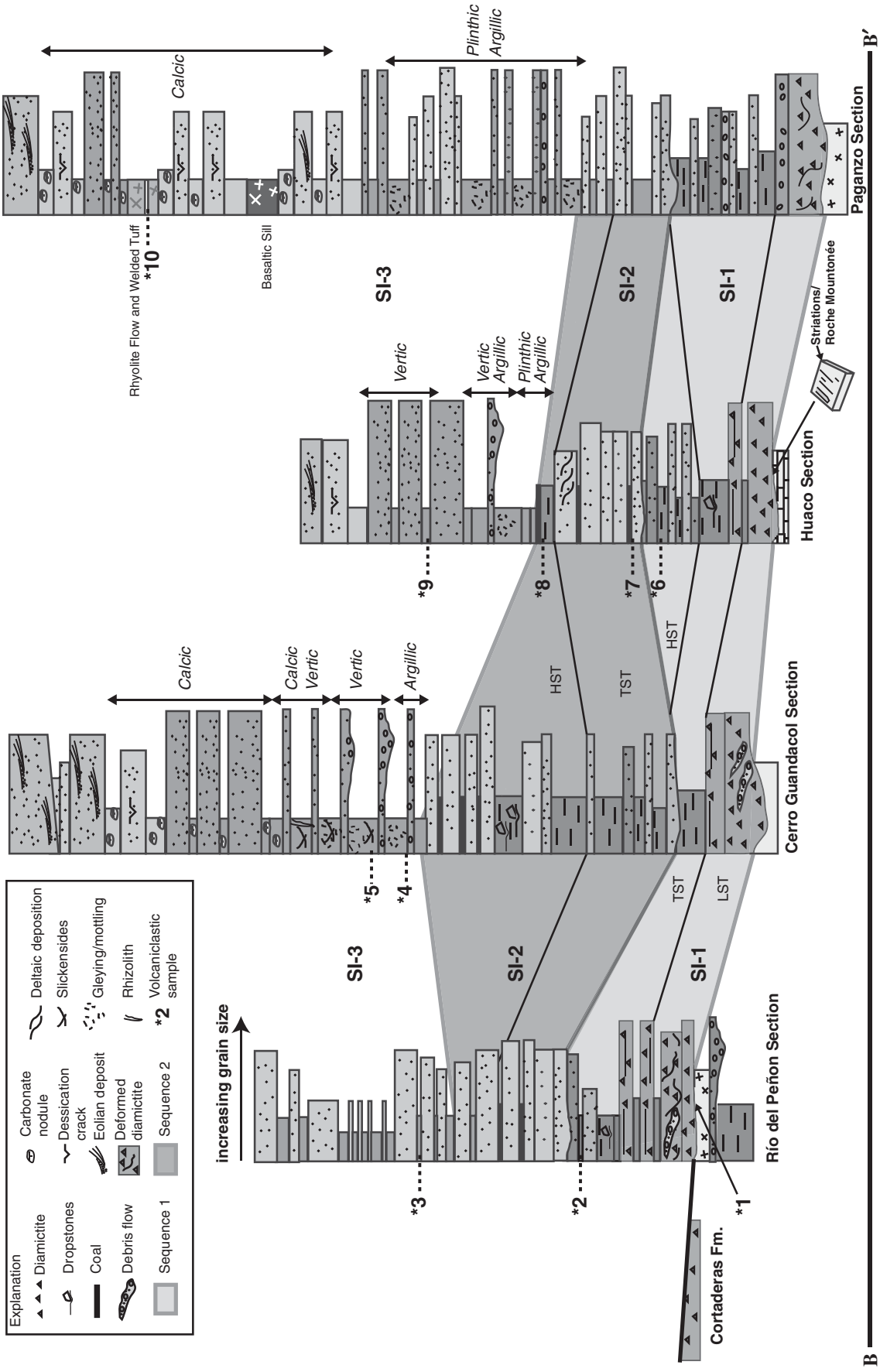

Figure 6. Summary of measured stratigraphic sections used in this study from B to B′ (Fig. 1). Shaded regions denote sequence stratigraphic interpretations of Pazos (2002b) and Desjardins et al. (2009), for SI-1 and SI-2. LST—lowstand systems tract, TST—transgressive systems tract, HST—highstand systems tract. Calcic, Plinthic, Argillic, and Vertic denote dominant soil orders (Calcisols, plinthic Protosols, Argillisols, and Vertisols, respectively) referenced in the text and Table 3. *1—07VD-36, *2—07VD-35, *3—RPTIgn-1, *4—GPIgn-1, *5—07VD-26, *6—07VD-13, *7—07VD-5, *8—07VD-6, *9—07VD-8, *10—PPAsh-1.

TABLE 2. COMPARISON OF STAGE BOUNDARY AGES

Stratigraphic stage	GTS* 2004 (Ma)	Menning et al. (2006) (Ma)	Ogg et al. (2008) (Ma)	Davydov et al. (2010) (Ma)
Base Gzhelian	303.9	302	303.4	303.2
Base Kasimovian	306.5	305	307.2	306.6
Base Moscovian	311.7	312	311.7	314.6
Base Bashkirian	318.1	320	318.1	322.8
Base Serpukhovian	326.4	326.5	328.3	330.0
Base Visean	345.3	345.5	345.3	346.3
Base Tournaisian	359.2	358	359.2	359.2

Note: Stage boundaries reflect various biostratigraphic correlations and radiometric ages.
*Geologic time scale (GTS) from Gradstein et al. (2004).

between diamictites of SI-1 and the underlying rocks (e.g., Ordovician San Juan Limestone), striations (Fig. 7E), roche moutonnee, nail-head striations, and polished surfaces have been observed on the underlying bedrock. The overlying diamictite facies include matrix-supported, massive and stratified diamictites (Dmm and Dms, respectively; cf. Eyles et al., 1983). Clast composition, in general, is dominated by metamorphic and granitic clasts with minor proportions of quartzite clasts. These clasts display facets and parallel striations and occur either in laterally continuous beds or as separate clusters of clasts separated by finer-grained mixed mud and sand-sized matrix. Mud rip-up clasts are observed in the uppermost diamictite at the Huaco locality. Clast-supported diamictites (Dcs) occur as laterally discontinuous beds displaying lenticular morphology. Clast-supported conglomerates and trough cross-bedded and ripple-laminated sandstones also occur intermixed with diamictites (Dcs, Dmm, or Dms) or bedded in vertical association with diamictites. Internal deformation in the form of large (tens to hundreds of meters) slumps and slide blocks is abundant within the Dmm and Dms facies (Fig. 7D). The thickness of the diamictites is variable and ranges from several meters to hundreds of meters.

The aforementioned surficial features (e.g., striations, polish) preserved at the contact of SI-1 and older rock units implies glacial denudation and abrasion of the bedrock prior to the deposition of the diamictites, highlighting the role of glacial erosion in the formation of the large-scale (>100 m) erosive contacts between SI-1 and the underlying rock units (Limarino et al., 2006; Henry et al., 2008). However, at the Río del Peñon section, the glacigenic strata rest on weathered andesite, suggesting that some valley surfaces were not overrun by ice. The internal architecture of clasts in Dmm and Dms diamictites suggests deposition by rainout from meltwater plumes and icebergs or from subaqueous debris flows (Anderson et al., 1991). Dms facies in particular may reflect more open-marine conditions with sediment delivery through ice-rafting or meltwater plumes (Dowdeswell et al., 2000). The incorporation of angular boulders in Dmm facies indicates a high-relief source delivering texturally immature debris to the glacier via mass wasting (Matsch and Ojakangas, 1991). Parallel striations on subrounded clasts indicate a subglacial origin (i.e., lodgment till, lee-side till) of the sediment, reworked and rounded in a proglacial environment (Boulton, 1978). Clumps and clusters of clasts may indicate dump structures from debris-laden icebergs, which are typical of valley or outlet glaciers originating from mountains (Thomas and Connell, 1985; Syvitski, 1989; Cowan and Powell, 1991). Dropstones are common within these deposits (Fig. 7C). The occurrence of dropstones, grooves, and striations within beds (iceberg keel marks) indicates the importance of debris-laden icebergs within the depositional environment. Together, the lateral and downdip extent of Dms and Dcs facies indicates extensive collection of transitional glacimarine sediments in a valley or fjord setting, consistent with sediment delivery from valley or outlet glaciers denuding coastal mountains and supplying abundant englacial debris to a subaqueous, marine environment (Matsch and Ojakangas, 1991).

A glaciterrestrial affinity is proposed for at least the basal-most diamictite at the Huaco locality (Pazos, 2002b; Marenssi et al., 2005; Henry et al., 2008). The noted absence of marine fossils in the diamictite, coupled with striated boulder pavements and internal deformation, implies a subglacial, glaciterrestrial depositional environment for these deposits. However, basal diamictites of SI-1 further to the east (landward; Paganzo section) also display internal deformation, absence of striated pavements, and normal grading, indicating a subaqueous environment during deformation with syndepositional deformation in the form of slumping. Together, these sedimentary features indicate a variety of glacimarine and glaciterrestrial environments in the proto-Precordilleran region (Henry et al., 2008). Some conglomerates and sandstones were likely deposited as ice contact deltas or subaqueous outwash fans from underflow currents (Stewart, 1991), as evidenced by inclined beds of ripple-laminated sandstones abruptly transitioning to matrix-supported diamictite, and a localized lateral occurrence (<100 m). The geometry of the sandstones and proximity to Dmm facies suggest deposition via a turbulent jet emanating from a glacier. The observed internal deformation of the diamictites suggests deposition of water-saturated deposits across high-relief surfaces, characteristic of modern fjords. Alternatively, deformation of a diamictite can occur in the subglacial environment, as demonstrated by the work of Marenssi et al. (2005).

Acritarchs and brachiopod fossils have been observed in SI-1 strata overlying the diamictites, implying marine conditions (Gutiérrez and Limarino, 2001). Freshwater trace fossil assemblages within these deposits (Buatois et al., 2006) suggest periods of brackish conditions (Pazos, 2002a) created by freshwater release during glacial ablation and/or estuarine circulation and are consistent with a fjord depositional environment. Ice-flow directions inferred from measurements on glacial striations located on basement rocks and soft-sediment surfaces within the glacigenic strata suggest radial ice flow away from the proto-Precordillera (López-Gamundí and Martinez, 2003; Henry et al., 2008).

The palynology of the diamictite-bearing rock units suggests a temporal distinction between diamictites of the Cortaderas Formation and diamictites of SI-1 (Guandacol Formation and equivalents). Diamictites in the Cortaderas Formation (Fig. 4; Angualasto Group) contain palynomorphs of Visean age (César and Limarino, 1992; Perez Loinaze, 2007). The *Verrucosisporites quasigobbettii* and *Reticulatisporites magnidictyus* miospore biozone present in the Cortaderas Formation and absence of monosaccate pollen confirm the Visean age of this stratigraphic unit (Perez Loinaze, 2007). A Namurian (Serpukhovian to Bashkirian) age for the overlying SI-1 diamictites has been previously established by palynomorphs and terrestrial floral assemblages, which include the first appearance of pollen in Paleozoic diamictites in the region (Archangelsky et al., 1987; César and Gutiérrez, 2000; Limarino et al., 2002).

The stratigraphic relationships (Figs. 6 and 8), distinct palynomorph associations, and the U-Pb ages reported here record two glacial events during the Mississippian in northwest Argentina: Visean diamictites of the Cortaderas Formation and the Serpukhovian to Bashkirian diamictites of SI-1 (Guandacol Formation and equivalent units). Both diamictite-bearing rock units are exposed near the Río del Peñon locality (Fig. 1). The older diamictites of the Cortaderas Formation occur beneath an erosional surface, above

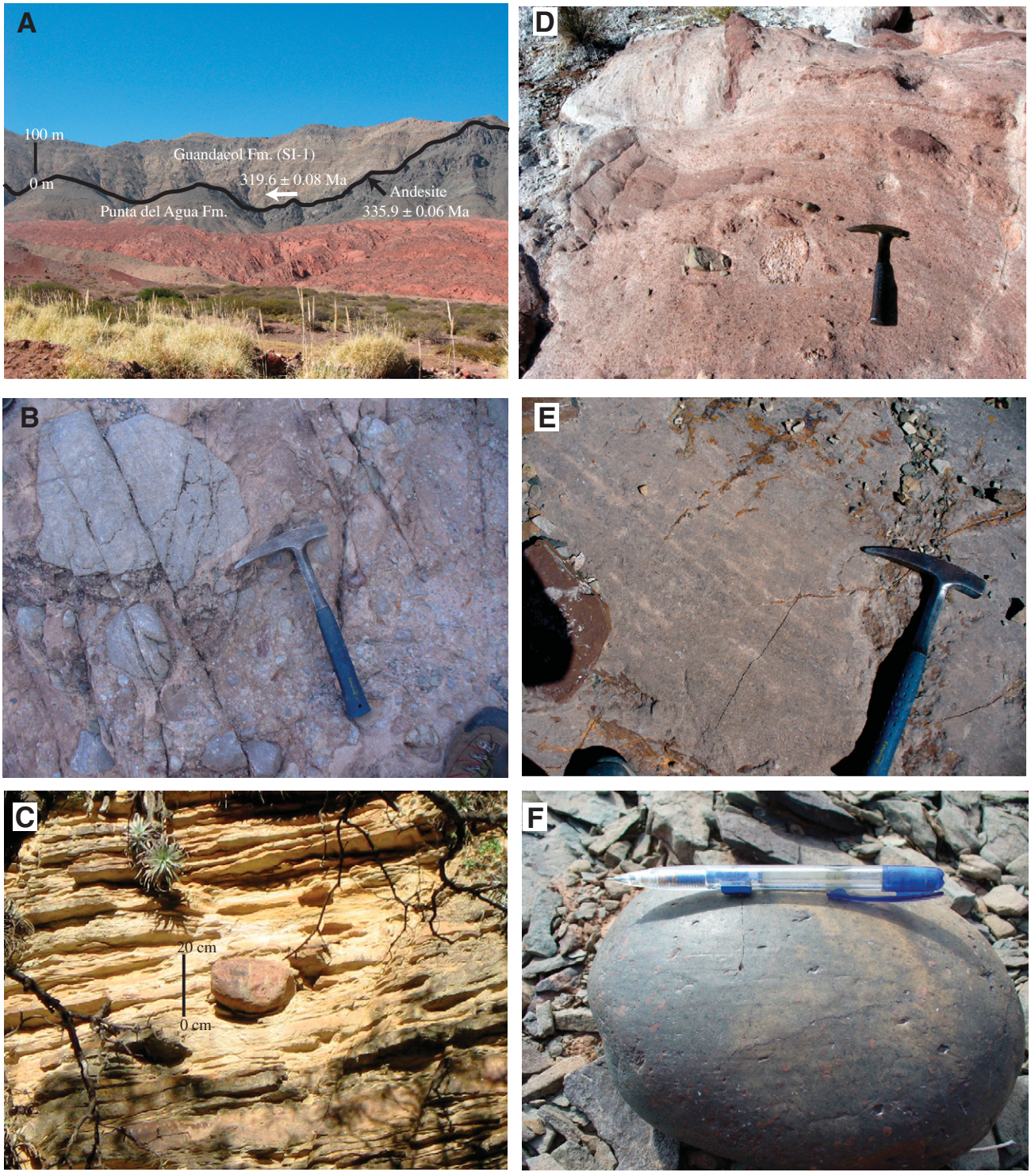

Figure 7. (A) Erosional contact between the Punta del Agua and Guandacol Formations. The Punta del Agua Formation occurs as darker-colored strata beneath the black line; a black arrow pointing to the highlighted surface indicates the approximate position of a dated sample from the Punta del Agua Formation; a white arrow within the Guandacol Formation points to the approximate position of a dated sample from the postglacial transgressive facies of SI-1. (B) Basal diamictite of SI-1 composed of Ordovician San Juan Limestone at the Huaco section. (C) Dropstone (center of picture) in the postglacial transgressive facies of SI-1; the dropstone clearly depresses the underlying turbiditic sediments. (D) Deformed basal diamictites of SI-1. (E) Glacial striations on the flat and polished surface of the Ordovician San Juan Limestone at the contact with the limestone and the overlying diamictites of SI-1. (F) Outsized clast found in distal deltaic facies in SI-2; slight striations are observed on the clast in the orientation of the pencil.

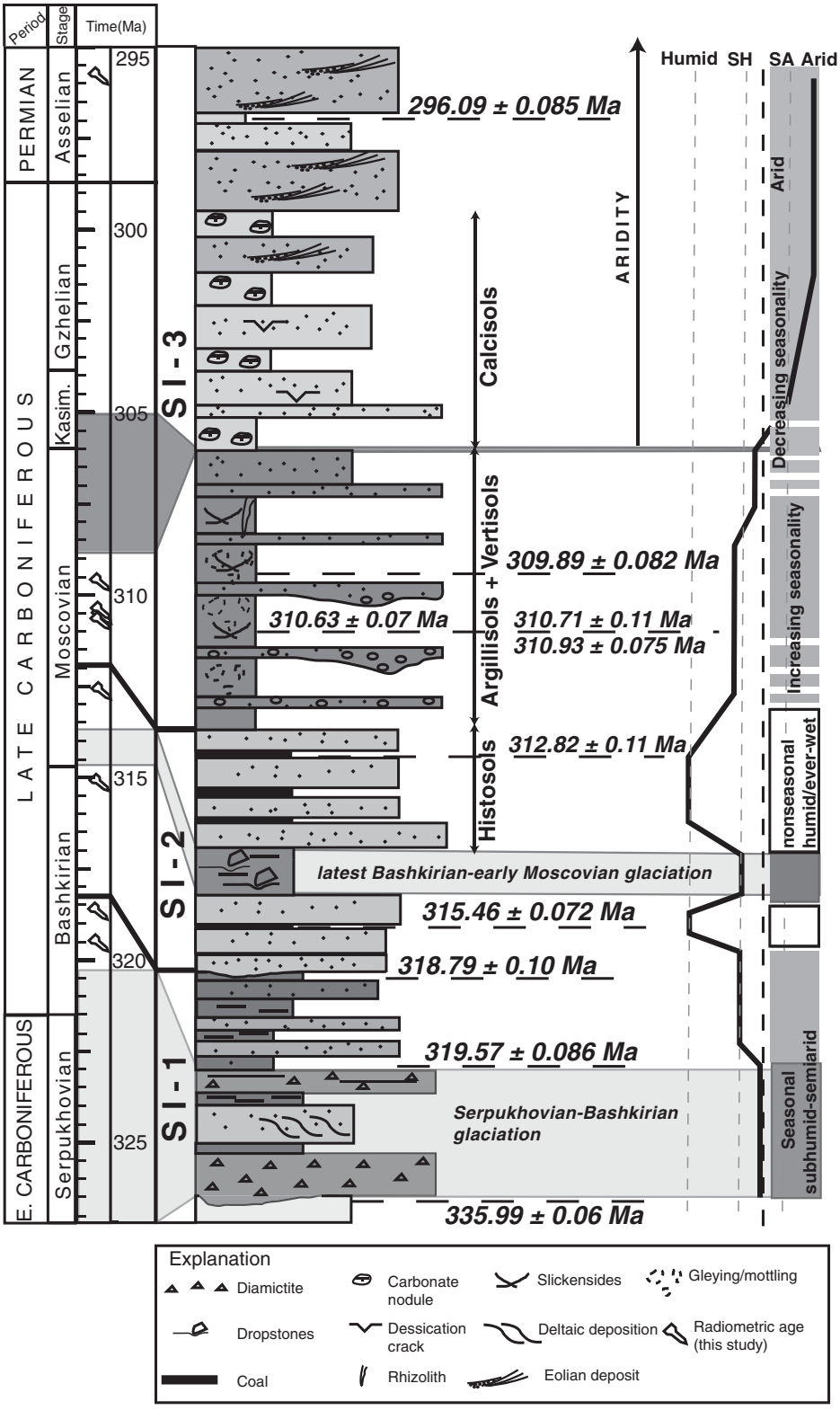

Figure 8. Composite stratigraphic column for the Paganzo Group. Light-gray shading indicates the SI-1 and SI-2 glacigenic deposits. Lithostratigraphic bounding surfaces on the stratigraphic column are shown by dark shaded bands extending to the time scale. Predominant soil orders are shown with their stratigraphic extent indicated by the vertical arrows. Inferred seasonality and precipitation/effective soil moisture are shown on far left. See text for a discussion of the inferred paleoclimate trends. SH—subhumid; SA—semiarid.

which diamictites of SI-1 are exposed (Fig. 3B). Along strike, the Cortaderas Formation is not exposed, and time-equivalent andesites interbedded with conglomerates of the Punta del Agua Formation are unconformably overlain by diamictites of SI-1. A 335.99 ± 0.06 Ma U-Pb age from an andesite in the uppermost Punta del Agua Formation (laterally equivalent to the Cortaderas Formation) in contact with diamictites of SI-1 is consistent with a mid-Visean age for the first stage of glaciation recorded in northwestern Argentina. A 319.57 ± 0.09 Ma U-Pb age from the postglacial transgressive facies of SI-1 (Guandacol Formation) provides a minimum age constraint on the second phase of glaciation.

Mid-Visean glacial events are recorded elsewhere on Gondwana; the best-documented deposits occur in the Poti Formation of the Parnaíba Basin (Fig. 1), the Faro Formation of the Amazon Basin (Fig. 1), and the Jandiatuba Formation of the Solimões Basin (Caputo, 1985; Caputo et al., 2008; Rocha Campos et al., 2008). Contemporaneous diamictites of equivocal glacial affinity also occur in the Witteberg Group of the main Karoo Basin, South Africa (Streel and Theron, 1999; Isbell et al., 2008b). Additionally, eustatic fluctuations of 10–50 m inferred from paleovalley incisions and cyclic stacking patterns within shallow-marine successions throughout paleotropical Euramerica (Horbury, 1989; Wright and Vanstone, 2001; Smith and Read, 2000, 2001; Bishop et al., 2009) have been argued as far-field (paleotropical) evidence for the onset of late Paleozoic glaciation as early as the mid-Visean.

A maximum Namurian age (329 Ma to 319 Ma; Davydov et al., 2010) for this glacial event is less well constrained by palynomorphs in shales near the base of SI-1 (Archangelsky et al., 1987; Césari and Gutiérrez, 2000). Serpukhovian-aged strata have been recently documented west of the Huaco locality (Balseiro et al., 2009) and further constrain the base of SI-1 to the late Serpukhovian or younger. These relationships indicate an estimated range of 323 Ma to 319.57 ± 0.09 Ma for glacigenic sediments of SI-1 (Guandacol Formation and equivalent units), which coincides with the C2 glacial event documented from eastern Australia (Fielding et al., 2008a).

Based on stratigraphic relationships and the two reported U-Pb ages, an unconformity of ≥12 m.y. occurs between the Angualasto Group (Cortaderas Formation and equivalent units) and the Paganzo Group (SI-1). The overlap in timing of the unconformity with the development of the Paganzo Basin during the late Mississippian (Limarino et al., 2006) suggests, in part, a tectonic control for the onset of this

unconformity. This further confirms the occurrence of two discrete glacial events in this region of southwestern Gondwana, in marked contrast with existing Permian-Carboniferous paleogeographic reconstructions and climate models, which indicate widespread continental glaciation emanating from this region in the Visean and extending well into the Permian (Frakes et al., 1992). Furthermore, both glacial events recorded in the study area likely occurred as alpine-dominated glaciations, as suggested by lateral discontinuity of glacigenic diamictites within paleovalleys and an inferred mountainous sediment source. Notably, complete ablation of alpine ice between glaciations would have contributed minimally to glacio-eustasy (Isbell et al., 2003, 2008b).

Stratigraphic Interval 2 and Equivalent Units

SI-2 strata (Tupe Formation and equivalent units) have been interpreted (Pazos, 2002a; Limarino et al., 2002; Desjardins et al., 2009) as postglacial progradational to aggradational fill in the Paganzo and Río Blanco Basins deposited during an initial marine transgression following a forced regression (Limarino et al., 2006). SI-2 unconformably overlies SI-1 in the Río Blanco Basin, transitioning landward into a correlative conformity in the central-eastern Paganzo Basin (Limarino et al., 2006; Henry et al., 2008). Lower SI-2 strata consist of multistory fluvial sandstones and well-sorted, tabular-bedded sandstones (Fig. 6) that are interpreted to be upper shoreface marine deposits (Desjardins et al., 2009). Progradational to aggradational coal-bearing fluvio-deltaic deposits overlie SI-2 strata (Limarino et al., 2006).

The presence of the Nothorhacopteris, Botrychiopsis, Ginkophyllum (NBG) zone flora in coals (Histosols) of SI-2 and low-diversity lycophytes, sphenophytes, pteridosperms, Cordaitales, and progymnosperms has been argued as evidence for a Pennsylvanian age for the Tupe Formation in the study area (Archangelsky et al., 1987; Gutiérrez and Limarino, 2006). Palynomorphs (*Raistrickia densa–Convolutispora muriornata*) in coals and black shales of the Tupe Formation could extend the age to the Stephanian (Kasimovian) or younger (López Gamundí et al., 1997; Césari and Gutiérrez, 2000). U-Pb ages of two ashes from the upper SI-2 strata reported here (315.46 ± 0.07 Ma and 312.82 ± 0.11 Ma), however, constrain SI-2 (Tupe Formation and equivalent units) strata to an early Moscovian minimum age (Table 1; Figs. 6 and 8).

In this paper, we report the occurrence at the Cerro Guandacol locality of a previously unrecognized dropstone-bearing interval, suggesting the possibility of a third glacial event during the Pennsylvanian in this region of southwestern Gondwana. Dropstones, which range in size from pebbles to cobbles, occur as "outsized" clasts in laterally continuous, thin-bedded, fine-grained micaceous sandstones displaying planar bedding and rare cross-lamination. The "outsized" clasts occur as a variety of compositions (metamorphic lithologies) but are predominantly granitic in composition, subangular to subrounded, and in some cases display facets or striations (Fig. 7F). Truncations and depressions of laminae are observable around clast margins (Fig. 7C), and these clasts occur as laterally equivalent clusters with spatial variability in the density of clast clustering.

The disparity in grain size between the "outsized" clasts and finer-grained matrix implies a "hydrodynamic paradox" (Bennett et al., 1996a), and the truncation of laminae suggests vertical emplacement of these clasts (Thomas and Connell, 1985). Dropstones, by themselves, are equivocal indicators of paleoclimate (Bennett et al., 1994; Bennett and Doyle, 1996; Donovan and Pickerill, 1997), as many depositional mechanisms have been ascribed to these deposits that bear no control from the ambient climatic conditions (e.g., tree rafting, turbidites, flotation, projectile). However, the observation of clast clustering, angularity, striations, and facets on clasts, and incorporation of several clast lithologies, indicates a depositional mechanism of glacial affinity (i.e., ice rafting, iceberg dump). The $^{206}Pb/^{238}U$ ages (315.46 ± 0.07 Ma [2σ] and 312.82 ± 0.11 Ma [2σ]) from tonsteins above and below the dropstone interval in SI-2 provide a latest Bashkirian to early Moscovian age for this potential third interval of glaciation, which has been previously undocumented in this region. Notably, this interval coincides with the most extensive Pennsylvanian glacial event (C4) recorded in eastern Australia (Fielding et al., 2008a) and more widespread glaciation in the Parnaíba Basin (Brazil; Caputo et al., 2008), the basal glacigenic strata of the Dwyka Group (South Africa; Visser, 1989, 1991; Isbell et al., 2008a), and the Al Khlata Formation (Huqf area, Sultanate of Oman; Martin et al., 2008), suggesting possible widespread glaciation across Gondwana during the latest Bashkirian to early Moscovian (315–312 Ma).

Stratigraphic Interval 3 and Equivalent Units

The SI-3 (Patquia Formation and equivalent units) in the Río Blanco and Paganzo Basins is defined primarily by a major lithologic change between these and underlying SI-2 deposits. In the Río Blanco Basin, deltaic deposits of SI-2 are juxtaposed against lower shoreface facies of SI-3 (Net and Limarino, 2006). Progradational shoreface facies directly overlie the transgressive facies of the SI-2 and SI-3 contact (middle and upper Río del Peñon Formation) and transition to deltaic and terrestrial facies in the middle and upper strata of SI-3 (Net and Limarino, 2006). In the Paganzo Basin, the base of SI-3 is demarcated by an abrupt change in fluvial style from multistory channels that characterize SI-2 strata to anastomosing and braided stream deposits of SI-3 (Limarino et al., 2006). The upper Patquia Formation (SI-3) is composed of eolian, ephemeral stream, and playa-lake deposits (Limarino and Spalletti, 1986; López-Gamundí and Breitkreuz, 1997; Limarino et al., 2006).

SI-3 (Patquia Formation and equivalent units) has been traditionally assigned an Early to Late Permian age based on the occurrence of Gangamopteris and Glossopteris megaflora and the pollen biozone *Protohaploxypinus*, which has an estimated age range of Asselian–Sakmarian (Césari et al., 2007). The middle and upper strata of SI-3 have been interpreted as recording the long-term Permian aridification trend, recognized in Pangean deposits worldwide (Parrish, 1993).

U-Pb ages for basal SI-3 strata (310.73 ± 0.12 Ma, 310.93 ± 0.08 Ma, and 309.89 ± 0.08 Ma), coupled with estimated long-term sediment accumulation rates, provide constraints for the onset of aridity in the Paganzo Basin. U-Pb ages from the basal strata of SI-3 indicate long-term average sediment accumulation rates for fluvial facies between ~90 m/m.y. and 105 m/m.y. Taking into account the limitations of the assumption of constant long-term sedimentation rates, a broad estimate for the onset of aridity of between 305 and 309 Ma (mid-Moscovian to earliest Kasimovian) can be made. The U-Pb age of upper eolian strata of SI-3 (296.09 ± 0.08 Ma) further constrain the onset of aridity to the latest Pennsylvanian (between 306 and 303 Ma) by linear extrapolation down section to the initial semiarid to arid strata, using long-term average sediment accumulation rates estimated for eolian facies (~55 m/m.y.).

K-Ar ages (302 ± 6 Ma and 288 ± 7 Ma) on basalts, which intrude SI-3 strata, from the central Paganzo Basin and from basaltic intrusions in the Río Blanco Basin (Coughlin, 2000) indicate emplacement of basalt in the late Pennsylvanian or Early Permian, thus providing a minimum age for SI-3 in the modern Andean Precordilleran region (Thompson and Mitchell, 1972). Furthermore, our U-Pb age of 296.09 ± 0.08 Ma supports previous indication of an Early Permian minimum age for deposition for SI-3 strata in the modern Andean Precordillera.

PALEOCLIMATE RECONSTRUCTION FOR SW ARGENTINA

Paleosols in SI-2 and SI-3 strata were measured and described on a centimeter scale, focusing on down profile and lateral accumulation of secondary minerals, horizonation, rooting structures, destruction of bedding fabric, and mottling or gleying. Master horizons (e.g., O, E, A, B, C) were determined for these paleosols, and classification of soil order and soil horizons followed the approach of Mack et al. (1993) and the Soil Survey Staff (2006). Descriptions and horizon classification are found in Table 3. Results are summarized here and integrated with the U-Pb ages and other climate-sensitive sedimentary facies to further refine the nature and timing of climatic shifts in this region. While these climatic parameters are difficult to establish from soil morphology alone (Dahms and Holliday, 1998), changes in paleoclimate conditions are inferred from morphologies in conjunction with observed changes in landscape position, stratigraphic variation in fluvial sedimentation style, and changes in parent material. Protosols, which are widespread in the Paganzo Group, are not considered in the paleoclimate reconstruction, given that they are equivocal indicators of paleoclimate (Mack et al., 1993).

STRATIGRAPHIC INTERVAL 2

U-Pb ages reported here constrain the oldest preserved paleosols of SI-2 to ca. 315 Ma, whereas the ages of the youngest paleosols are undefined. In general, paleosols in SI-2 strata can be grouped into three types, organic paleosols, paleosols with an argillic subsurface horizon, and pedogenic Fe-bearing paleosols.

Organic paleosols are preserved as thin coals in the lower and middle portions of SI-2 at every locality used in this study. Coals underlie and overlie the dropstone-bearing interval constrained by U-Pb zircon ages to between 315 and 312 Ma (Fig. 8). These soils are marked by the presence of organic matter constituting over 80% of a horizon, and they are underlain by mineral material that is often bluish gray in coloration (Table 3). Organic constituents are the most variable component of these soils, and in most cases, they are lithified to bituminous coal. However, in some cases, plant debris can be identified. Organic paleosols are found within laterally continuous quartzofeldspathic medium-grained and moderately sorted sandstones, as well as thin-bedded fine-grained quartzose sandstones and siltstones.

The percentage of organic matter within these horizons indicates that they are O master horizons (sensu Soil Survey Staff, 2006), which overlie gleyed mineral horizons (Cg), indicating these soils are Histosols. Histosols occur where the influx of organic material to a surface exceeds the decomposition rate of organic matter (Rabenhorst and Swanson, 2000; Buol et al., 2003). This requirement is achieved in saturated conditions that can occur in coastal plain and deltaic environments, and generally in water-saturated landscapes (e.g., fens, bogs, pocosins). Coastal plain and deltaic environments are consistent with the interpreted depositional setting of Histosols of the Paganzo Group.

Paleosols containing a well-developed argillic horizon occur in the uppermost Tupe Formation and are younger than 312.8 Ma. These soils are found at the Huaco, Cerro Guandacol, and Paganzo localities (Fig. 1; Table 3). A typical paleosol profile for this group has upper horizons that lack bedding, a well-developed soil structure (e.g., angular blocky structure), and horizonation with reddish coloration, mottling, and horizontal to subhorizontal burrows. These soils are characterized by a marked increase in clay percentage in subsurface horizons relative to overlying eluvial horizons, evidenced by clayey grain bridges, and particle coatings define argillic horizons in these paleosols. Mn coatings (Table 3) were observed on some clasts and clay bridges and had a positive reaction with 30% H_2O_2. The basal horizon is composed of labile material (biotite and muscovite) and contains crude lamination. These paleosols occur among finely laminated and thin-bedded siltstones with fine-grained sandstone interbeds. Lenticular, arkosic, and moderately sorted sandstones occur laterally from these paleosols.

Gley features (Mn coatings) permit classification of the upper horizons as Bwg master horizons. The underlying horizons are classified as Btg horizons, reflecting the illuvial accumulation of clay and redoximorphic features (Vepraskas, 1994). The displacement and bridging of grains within a subsurface horizon are indications of illuvial transport of clay-sized particles, which is requisite for the formation of an argillic horizon (Southard and Southard, 1985). The presence of an argillic horizon and gleying indicates well-drained soil conditions and allows classification of these paleosols as Argillisols (Mack et al., 1993). Precipitation and soil moisture are central to the development of argillic horizons (Elliott and Drohan, 2009), and argillic horizons can form over a wide range of moisture regimes (Buol et al., 2003). However, the absence of carbonates and minerals more soluble than calcite in these argillic horizons indicates a subhumid to humid moisture regime. The sediments surrounding these soils are interpreted as fluvial and floodplain facies of single-story avulsive fluvial channels with some crevasse splay deposits.

Plinthic paleosols are characterized by red to dark red coloration with moderate to extensive gleyed coloration and the accumulation of Fe-(oxy)hydroxide nodules as either discrete nodules (~1–3 mm diameter) or as an indurated polygonal Fe-cemented horizon in the lower horizons of the paleosol. These paleosols are very common at the Huaco and Paganzo localities (Fig. 1). Plinthic paleosols occur in thin-bedded siltstones and lenticular arkosic sandstones that display erosive lower contact, truncating underlying siltstones and claystones. These paleosols are laterally discontinuous at the meter scale and occur adjacent to the lenticular sandstone bodies. Indurated Fe-cemented horizons are commonly found within finely laminated siltstones and carbonaceous siltstones.

The morphology of the Fe in these horizons indicates a Bv horizon for the nodular Fe-bearing horizon and a Bsm horizon for the indurated polygonal Fe-bearing horizon (Soil Survey Staff, 2006). The underlying horizons display weak pedogenic features and are characterized as C horizons. The dominant pedogenic processes inferred from these soils are gleying (Kaczorek et al., 2004) and the persistent oxidation of Fe in the upper portion of the soil pedon. The lack of pedogenic alteration within a soil containing a Bv horizon permits classification as plinthic Protosol (Mack et al., 1993). The Bsm horizon closely matches the Raseneisensteins of eastern and northern Europe (Kaczorek et al., 2004) or bog irons of the eastern coastal plain of the United States (Crerar et al., 1979), indicating the importance of a sustained high water table in imposing a "permanent" redox barrier to sequester redox-sensitive elements. The latter permits classification of this soil type as a plinthic Gleysol (Mack et al., 1993).

The predominance of Argillisols coeval with Histosols and plinthic Protosols in the stratigraphic interval overlying the dropstone-bearing interval of SI-2 strata indicates that a humid to ever-wet paleoclimate continued into the latest Bashkirian (Fig. 8).

STRATIGRAPHIC INTERVAL 3

Paleosols in SI-3 strata can be grouped into two paleosol groups: (1) calcic argillic horizon–bearing soils, and (2) carbonate-bearing soils. Calcic argillic horizon–bearing soils dominate in the lower SI-3 strata, and carbonate-bearing soils predominate in the middle and upper portions of SI-3 strata. Overall, the occurrence of pedogenic carbonate in these paleosols implies a decrease in soil leaching and a decrease in effective soil moisture delineating a trend toward

TABLE 3. SUMMARY OF PALEOSOL DESCRIPTIONS

Locality	Formation	Soil order	Thickness (cm)	Horizon	Description
Río del Peñon	Middle Río del Peñon	Histosol	0–20	O	85% organic matter, lithified bituminous coal, clear and sharp upper and lower boundaries
			20–25	Cg	Bluish gray silty mudstone, massive, wavy sharp lower boundary, minor yellowish orange mottles
Paganzo	Patquia	Argillisol	0–15	Btg	Reddened clay matrix displacing quartz and lithic clasts. Clay bridges between quartz grains 30%, Mn-coatings on clasts, clear sharp upper boundary, wavy sharp lower boundary
			15–24	BC	Grain-to-grain contact, relict bedding, 10% clay infilling pore spaces, clear sharp lower boundary, lenticular bedding morphology
Huaco	Upper Tupe Fm.	Plinthic Gleysol	0–5	E	Yellowish white quartzose sandstone, massive, wavy diffuse upper boundary, wavy sharp lower boundary
			5–70	Bsm	Extremely firm, iron cemented, voids 5% filled with clay and sand-sized particles, metallic luster on some surfaces, occurs as isolated pods, clear sharp lower boundary
			70–100	Bw	Reddened matrix, relict bedding, micaceous sandstone with carbonaceous debris, diffuse lower boundary
Guandacol	Patquia Fm.	Calcic Vertisol	0–15	Bssk1	Mottled maroon 75% greenish gray 25% color, 20% clay, slickensides, antithetic slickenside planes, wedge-shaped aggregates, 5% carbonate nodules, wavy sharp lower boundary, upper boundary undefined
			15–115	Bssk2	Mottled maroon and greenish gray color, 25% clay, antithetic slickensides, long (>5 cm) elongate carbonate nodules, wedge-shaped aggregates
			115–165	Cr	Dusky red colored, 10% clay, relict bedding, micaceous sandstone
Guandacol	Patquia Fm.	Calcisol	0–6	Bk1	Red colored, thin (0.5 cm diameter) intertwined carbonate stringers, laterally expansive, micaceous arkosic sandstone
			6–11	Bkm	Bluish gray mottles and greenish gray carbonate, carbonate cemented, nodules, cracks, and circumgranular cements within cemented layer
			11–50	Bk2	Red color, large (>3 cm diameter) carbonate nodules, displacive, some coalesced nodules, massive micaceous arkosic sandstone
Guandacol	Patquia Fm.	Protosol	0–25	Bw	Reddened micaceous arkosic sandstone, single grain structure, greenish gray vertically branching mottles and spherical and tubiform mottling
			25–30	BC	Red color, relict bedding, micaceous arkosic sandstone

Note: Soil descriptions are from representative paleosol profiles in the study area.

increased aridity throughout the SI-3 interval (Fig. 8; Moscovian to Early Permian).

Carbonate- and argillic horizon–bearing soils exhibit three main subsurface horizons. The uppermost horizon contains wedge-shaped aggregate ped structures, an overall red coloration, and an accumulation of carbonate nodules and elongated tubular rhizoliths. The underlying horizon contains large antithetic slickensides (Tabor and Montañez, 2005), and wedge-shaped aggregates. The basal horizon is composed of low-angle antithetic slickensides and angular blocky soil structure. Paleosols of this type are found primarily at the Cerro Guandacol locality and to a lesser extent at the Huaco locality. These soils occur predominantly within medium- to fine-grained arkosic silty sandstones adjacent to lenticular arkosic sandstones and laterally continuous quartzofeldspathic sandstones.

The presence of wedge-shaped aggregates and slickensides is indicative of vertic soil structures (Soil Survey Staff, 2006). The combination of vertic features and pedogenic carbonate permits classification of Bssk horizons for the uppermost horizons of this soil type (Soil Survey Staff, 2006). The lower soil horizons are classified as Bss horizons due to the presence of vertic features. Vertic features are consistent with their formation by seasonal shrink and swell of expansible phyllosilicates driven by strong seasonality of precipitation (Mack et al., 1993; Driese et al., 2005). Increased seasonality and reduced effective soil moisture, when compared with Argillisols, are indicated by the presence of pedogenic carbonate, which is interpreted to have formed synchronously with the seasonal expansion and contraction of the soil, as these carbonate nodules are commonly bent along the sense of motion of the slickensides. Vertic structures and synchronous precipitation of pedogenic carbonate classify this soil as a calcic Vertisol (Mack et al., 1993).

Carbonate-bearing paleosols in SI-3 strata exhibit well-developed horizonation, fine to medium angular blocky ped structure, overall red coloration, and accumulation of carbonate nodules and rhizoliths. The upper horizon in these paleosols is deeply reddened, and it is underlain by a carbonate-rich horizon of nodules, coalesced nodules, or an indurated carbonate hardpan. Calcified roots (rhizoliths) are common in these paleosols and are restricted to the uppermost paleosol horizons. These paleosols are common at the Guandacol and Paganzo localities. These soils occur in the middle and upper portions of SI-3 strata in association with fine-grained, well-sorted quartzose sandstones with climbing ripple cross-stratification and pebble-lags at the base of bedding contacts.

The uppermost horizon containing rhizoliths is classified as a Bk horizon. The indurated carbonate layer is classified as a Bkm horizon (Soil Survey Staff, 2006), and the underlying horizons are classified as Bk horizons. The occurrence of pedogenic carbonate in subsurface soil horizons (petrocalcic horizon) is an indication of reduced leaching within the soil due to a net water deficit, usually where mean annual precipitation falls below 100 cm (Jenny, 1980). Carbonate nodules or hardpans are the primary observable form of pedogenic alteration (Wright and Tucker, 1991; Alonso-Zarza, 2003), and these soils are

classified as Calcisols (Mack et al., 1993), as calcification was the dominant soil-forming process. The occurrence of Calcisols in the Paganzo Group coeval with feldspar clast–rich braided fluvial deposits and playa-lake deposits indicates that these paleosols likely formed during a semiarid to arid paleoclimate.

The stratigraphic trend from calcic Vertisols to dominantly Calcisols in the middle portion of SI-3 strata indicates a shift from seasonal dry subhumid to semiarid conditions (inferred from the calcic Vertisols) to overall reduced effective soil moisture and likely nonseasonal semiarid to arid climate during the interval of deposition of the lower to middle strata of SI-3 (Fig. 8). A U-Pb age of 310.93 ± 0.08 Ma from Cerro Guandacol constrains this inferred climate shift to the middle to late Moscovian. The persistence of Calcisols into the early Kasimovian, constrained using long-term sediment accumulation rates, and the occurrence of eolianites and playa-lake facies in upper SI-3 strata indicate that nonseasonal arid conditions were well established in southwestern Gondwana by the late Pennsylvanian, significantly earlier than previously suggested for southern Gondwana (Limarino and Spalletti, 1986) and for the Pangean paleotropics (Parrish, 1993).

SUMMARY

High-precision U-Pb calibration of climate-sensitive sedimentary deposits (i.e., glacigenic deposits, fluvial-style deposits, paleosols, and eolianites) in the Paganzo Group permits significant refinement of the climate evolution of this region of southwestern Gondwana during the Permian-Carboniferous. The stratigraphic and sedimentologic relationships presented here define at least three episodes of glaciation in northwestern Argentina. The onset of this glaciation occurred in the mid-Visean, likely dominated by alpine glaciation in the proto-Precordillera region (Isbell et al., 2003; Limarino et al., 2006). A second glacial event spanned the Serpukhovian to early Bashkirian and was characterized by alpine glaciation and postglacial fjord-filling sedimentation. A likely third glacial event occurred in the mid-to-late Bashkirian through early Moscovian (315–312 Ma). Notably, the two Pennsylvanian glacial events were coincident with recently documented short-lived Pennsylvanian glaciations in eastern Australia (C2 and C4; Fig. 9; Fielding et al., 2008a, 2008b). Glacioeustasy reconstructed from penecontemporaneous paleotropical stratigraphic records (Serpukhovian through Bashkirian) indicate persistent high-magnitude fluctuations (50–90 m) from the mid-Carboniferous boundary through the middle to late Bashkirian

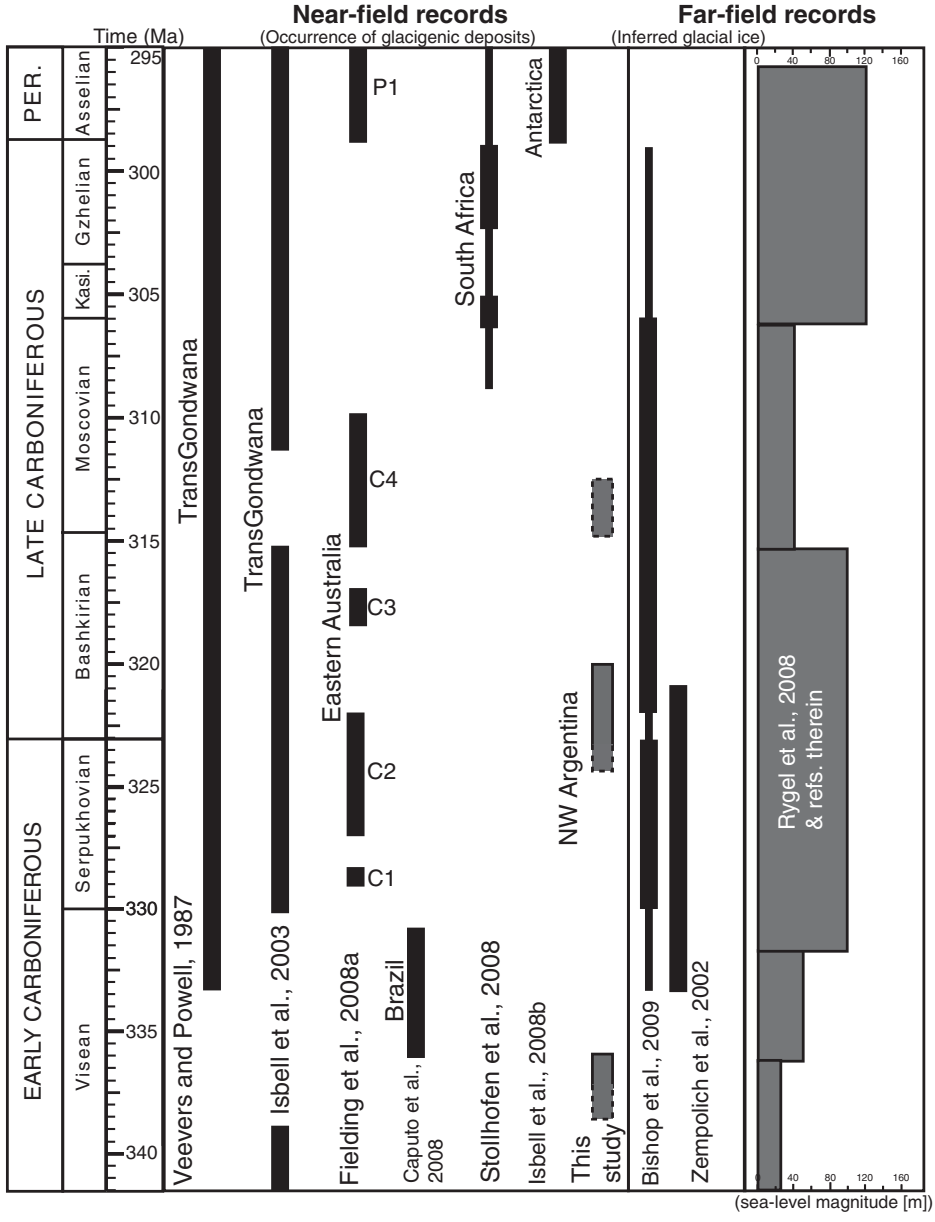

Figure 9. Near-field and far-field interpretations of the glacial history during the late Paleozoic ice age. The dashed box denotes the dropstone-bearing interval in the Paganzo Group as it may reflect distal ice-rafted deposits. The dashed portion of the Serpukhovian-Bashkirian glaciation reflects uncertainty in the constraints for the onset of this glaciation. The far-field interpretations of glacial history were reconstructed on the basis of glacioeustasy inferred from stratigraphic cyclicity and isotopic compositions of biogenic minerals.

(Fig. 9; Rygel et al., 2008). Significantly, despite the roughly coincident nature of inferred high-magnitude glacioeustasy with observed glacial events on Gondwana, the dominance of alpine glaciation inferred from stratigraphic architecture across Gondwana (Kneller et al., 2004; Limarino et al., 2006; Fielding et al., 2008a) could not have alone contributed significantly to this eustasy (Isbell et al., 2003).

The occurrence of Argillisols and Histosols in strata intercalated between the mid-Carboniferous boundary and early Pennsylvanian glacigenic deposits indicates that moist and seasonal climate conditions predominated at 45°S to 50°S paleolatitude (Fig. 8) during waning glaciation or nonglacial conditions throughout the latest Mississippian and early Pennsylvanian. A U-Pb calibrated shift in SI-3 paleosols from

calcic Vertisols to Calcisols indicates a major and relatively rapid (≤10^6 yr) decrease in seasonality and effective moisture. This inferred shift in precipitation occurred in the middle to late Moscovian and postdates all evidence for glaciation or coal-bearing intervals along the western margin of high-latitude (~50°S) Gondwana. The timing of the onset of aridity across the mid-to-late Pennsylvanian transition in the study region is coincident with a major climate shift from humid and subhumid to semiarid conditions recently documented throughout tropical Euramerica (Montañez et al., 2008; Bertier et al., 2008; Bishop et al., 2010).

ACKNOWLEDGMENTS

This manuscript benefited from the thoughtful reviews of two anonymous reviewers, which clarified the presentation of the stratigraphy and regional tectonics. We thank Associate Editor Fernando Corfu and one of the reviewers for comments on the U-Pb geochronology, which greatly improved the organization and presentation of our data. We thank Mike Eros, Cara Harwood, and Dan Horton for field assistance. We are grateful to Carina Colombi for logistical support. This work was supported by National Science Foundation (NSF) grants EAR-0545654, EAR-0650660, and OISE-0826105 to Isabel P. Montañez, and EAR-0521221 and EAR-0545247 to Mark D. Schmitz.

REFERENCES CITED

Alonso-Zarza, A.M., 2003, Palaeoenvironmental significance of palustrine carbonates and calcretes in the geological record: Earth-Science Reviews, v. 60, p. 261–298, doi: 10.1016/S0012-8252(02)00106-X.

Anderson, J.B., Kennedy, D.S., Smith, M.J., and Domack, E.W., 1991, Sedimentary facies associated with Antarctica's floating ice masses, *in* Anderson, J.B., and Ashley, G.M., eds., Glacial Marine Sedimentation; Paleoclimatic Significance: Geological Society of America Special Paper 261, p. 1–26.

Andreis, R.R., Archangelsky, S., Gonzalez, C.R., Lopez Gamundi, O., Sabattini, N., Acenolaza, F.G., Azcuy, C.L., Cortinas, J., Cuerda, A., and Cuneo, R., 1987, Cuenca Tepuel-Genoa, *in* Archangelsky, S., ed., El Sistema Carbonifero en la Republica Argentina: Cordoba, Argentina, Academia Nacional De Ciencias, p. 169–196.

Archangelsky, S., Azcuy, C.L., González, C.R., and Sabattini, N., 1987, V. Paleontologia, Bioestratigrafia y paleoecologia de las Cuencas Paganzo, Calingasta-Uspallata y Rio Blanco, *in* Archangelsky, S., Amos, A.J., Andreis, R.R., Azcuy, C.L., González, C.R., Lopez Gamundi, O., and Sabattini, N., eds., El Sistema Carbonifero en la Republica Argentina: Cordoba, Argentina, Subcommission Internacional del Carbonifero, Academia Nacional de Ciencias, p. 133–151.

Azcuy, C.L., Andreis, R.R., Cuerda, A., Hünicken, M.A., Pensa, M.V., Valencio, D.A., Vilasy, J.F., Archangelsky, S., Berkowski, D.A., and Leguizamón, R., 1987a, Cuenca Paganzo, *in* Archangelsky, S., ed., El Sistema Carbonifero en la Republica Argentina: Cordoba, Argentina, Academia Nacional De Ciencias, p. 41–100.

Azcuy, C.L., Arias, W., Cuerday, A., Andreis, R.R., and Archangelsky, S., 1987b, Cuenca San Rafael, *in* Archangelsky, S., ed., El Sistema Carbonifero en la Republica Argentina: Cordoba, Argentina, Academia Nacional De Ciencias, p. 153–168.

Balseiro, D., Rustán, J.J., Ezpeleta, M., and Vaccari, N.E., 2009, A new Serpukhovian (Mississippian) fossil flora from western Argentina: Paleoclimatic, paleobiogeographic and stratigraphic implications: Palaeogeography, Palaeoclimatology, Palaeoecology, v. 280, p. 517–531, doi: 10.1016/j.palaeo.2009.07.005.

Bennett, M.R., and Doyle, P., 1996, Global cooling inferred from dropstones in the Cretaceous: Fact or wishful thinking?: Terra Nova, v. 8, p. 182–185, doi: 10.1111/j.1365-3121.1996.tb00742.x.

Bennett, M.R., Doyle, P., Mather, A.E., and Woodfin, J.L., 1994, Testing the climatic significance of dropstones: An example from southeast Spain: Geological Magazine, v. 131, p. 845–848, doi: 10.1017/S0016756800012917.

Bennett, M.R., Doyle, P., and Mather, A.E., 1996, Dropstones: Their origin and significance: Palaeogeography, Palaeoclimatology, Palaeoecology, v. 121, p. 331–339, doi: 10.1016/0031-0182(95)00071-2.

Bertier, P., Swennen, R., Lagrou, D., Laenen, B., and Kemps, R., 2008, Palaeo-climate controlled diagenesis of the Westphalian C & D fluvial sandstones in the Campine Basin (north-east Belgium): Sedimentology, v. 55, p. 1375–1417, doi: 10.1111/j.1365-3091.2008.00950.x.

Bishop, J.W., Montañez, I.P., Gulbranson, E.L., and Brenckle, P.L., 2009, The Onset of Mid-Carboniferous Glacio-eustasy: Sedimentologic and Diagenetic Constraints, Arrow Canyon, NV: Palaeogeography, Palaeoclimatology, Palaeoecology, v. 276, p. 217–243, doi: 10.1016/j.palaeo.2009.02.019.

Bishop, J.W., Montañez, I.P., and Osleger, D.A., 2010, Dynamic Carboniferous climate change, Arrow Canyon, Nevada: Geosphere (in press).

Blakey, R.C., 2008, Gondwana paleogeography from assembly to breakup—A 500 m.y. odyssey, *in* Fielding, C.R., Frank, T.D., and Isbell, J.L., eds., Resolving the Late Paleozoic Ice Age in Time and Space: Geological Society of America Special Paper 441, p. 1–28.

Bodenbender, G., 1911, Constitución geológica de la parte meriodional de La Rioja y regions limítrofes: República Argentina: Academia Nacional de Ciencias, v. 19, p. 5–220.

Boulton, G.S., 1978, Boulder shapes and grain-size distributions of debris as indicators of transport paths through a glacier and till genesis: Sedimentology, v. 25, p. 773–799, doi: 10.1111/j.1365-3091.1978.tb00329.x.

Bowring, S.A., Grotzinger, J.P., Condon, D.J., Ramezani, J., Newall, M.J., and Allen, P.A., 2007, Geochronologic constraints on the chronostratigraphic framework of the Neoproterozoic Huqf Supergroup, Sultanate of Oman: American Journal of Science, v. 307, p. 1097–1145, doi: 10.2475/10.2007.01.

Buatois, L.A., Netto, R.G., Mángano, M.G., and Balistieri, P.R.M.N., 2006, Extreme freshwater release during the late Paleozoic Gondwana deglaciation and its impact on coastal ecosystems: Geology, v. 34, no. 12, p. 1021–1024, doi: 10.1130/G22994A.1.

Buol, S.W., Southard, R.J., Graham, R.C., and McDaniel, P.A., 2003, Soil Genesis and Classification (5th ed.): Ames, Iowa, Iowa State Press, 494 p.

Caputo, M.V., 1985, Late Devonian glaciation in South America: Palaeogeography, Palaeoclimatology, Palaeoecology, v. 51, p. 291–317, doi: 10.1016/0031-0182(85)90090-2.

Caputo, M.V., de Melo, J.H.G., Streel, M., and Isbell, J.L., 2008, Late Devonian and Early Carboniferous glacial records of South America, *in* Fielding, C.R., Frank, T.D., and Isbell, J.L., Resolving the Late Paleozoic Ice Age in Time and Space: Geological Society of America Special Publication 441, p. 161–173.

Césari, S.N., and Gutiérrez, P.R., 2000, Palynostratigraphy of Upper Paleozoic sequences in central-western Argentina: Palynology, v. 24, no. 1, p. 113–146, doi: 10.2113/0240113.

Césari, S.N., and Limarino, C.O., 1992, Palinomorfos Eocarboníferos en la Formación Cortaderas, provincia de San Juan, Argentina, *in* VII Simposio Argentino de Paleobotánica y Palinología, Corrientes: Asociación Paleontológica Argentina Publicación Especial 2, p. 45–48.

Césari, S.N., 2007, Palynological biozones and radiometric data at the Carboniferous-Permian boundary in western Gondwana: Gondwana Research, v. 11, p. 529–536, doi: 10.1016/j.gr.2006.07.002.

Condon, D.J., 2005, Progress report on the U-Pb interlaboratory experiment: Geochimica et Cosmochimica Acta, v. 69, p. 319.

Coughlin, T.J., 2000, Linked Orogen-Oblique Fault Zones in the Central Argentine Andes: The Basis of a New Model for Andean Orogenesis and Metallogenesis: [Ph.D. thesis]: Brisbane, University of Queensland, 207 p.

Cowan, E.A., and Powell, R.D., 1991, Ice-proximal sediment accumulation rates in a temperate glacial fjord, southeastern Alaska, *in* Anderson, J.B., and Ashley, G.M., eds., Glacial Marine Sedimentation; Paleoclimatic Significance: Geological Society of America Special Paper 261, p. 61–74.

Crerar, D.A., Knox, G.W., and Means, J.L., 1979, Biogeochemistry of bog iron in the New Jersey Pine Barrens: Chemical Geology, v. 24, p. 111–135, doi: 10.1016/0009-2541(79)90016-0.

Crowley, T.J., Hyde, W.T., and Short, D.A., 1989, Seasonal cycle variations on the supercontinent of Pangaea: Geology, v. 17, p. 457–460, doi: 10.1130/0091-7613(1989)017<0457:SCVOTS>2.3.CO;2.

Crowley, J.L., Schoene, B., and Bowring, S.A., 2007, U-Pb dating of zircon in the Bishop Tuff at the millennial scale: Geology, v. 35, no. 12, p. 1123–1126, doi: 10.1130/G24017A.1.

Dahms, D.E., and Holliday, V.T., 1998, Soil taxonomy and paleoenvrionmental reconstruction: A critical commentary: Quaternary International, v. 51/52, p. 109–114, doi: 10.1016/S1040-6182(97)00037-2.

Davydov, V.I., Crowley, J.L., Schmitz, M.D., and Poletaev, V.I., 2010, High-precision U-Pb zircon age calibration of the global Carboniferous time scale and Milankovitch-band cyclicity in the Donets Basin, eastern Ukraine: Geochemistry Geophysics Geosystems, doi: 10.1029/2009GC002736.

Desjardins, P.R., Buatois, L.A., Limarino, C.O., and Cisterna, G., 2009, Latest Carboniferous–earliest Permian transgressive deposits in the Paganzo Basin of western Argentina: Lithofacies and sequence stratigraphy of a coastal-plain to bay succession: Journal of South American Earth Sciences, v. 28, p. 40–53, doi: 10.1016/j.jsames.2008.10.003.

Donovan, S.K., and Pickerill, R.K., 1997, Dropstones: Their origin and significance: A comment: Palaeogeography, Palaeoclimatology, Palaeoecology, v. 131, p. 175–178, doi: 10.1016/S0031-0182(96)00150-2.

Dowdeswell, J.A., Whittington, R.J., Jennings, A.E., Andrews, J.T., Mackensen, A., and Marienfeld, P., 2000, An origin for laminated glacimarine sediments through sea-ice build-up and suppressed iceberg rafting: Sedimentology, v. 47, p. 557–576, doi: 10.1046/j.1365-3091.2000.00306.x.

Driese, S.G., Nordt, L.C., Lynn, W.C., Stiles, C.A., Mora, C.I., and Wilding, L.P., 2005, Distinguishing climate in the soil recorded using chemical trends in a Vertisol climosequence from the Texas Coast Prairie, and application to interpreting Paleozoic paleosols in the Appalachian Basin, U.S.A.: Journal of Sedimentary Research, v. 75, p. 339–349, doi: 10.2110/jsr.2005.027.

Dykstra, M., Kneller, B., and Milana, J.P., 2006, Deglacial and postglacial sedimentary architecture in a deeply incised paleovalley-paleofjord; the Pennsylvanian (late Carboniferous) Jejenes Formation, San Juan, Argentina: Geological Society of America Bulletin, v. 118, p. 913–937, doi: 10.1130/B25810.1.

Elliott, P.E., and Drohan, P.J., 2009, Clay accumulation and argillic-horizon development as influenced by aeolian deposition vs. local parent material on quartzite and limestone-derived alluvial fans: Geoderma, v. 151, p. 98–108, doi: 10.1016/j.geoderma.2009.03.017.

Eyles, N., Eyles, C.H., and Miall, A.D., 1983, Lithofacies types and vertical profile models; an alternative approach to the description and environmental interpretation of glacial diamict and diamictite sequences: Sedimentology, v. 30, p. 393–410, doi: 10.1111/j.1365-3091.1983.tb00679.x.

Fauqué, L., Limarino, C., Césari, S., and Sabattini, N., 1989, Hallazgo de Carbonifero inferior fosilifero en el Río de La Troya (Precordillera de La Rioja): Ameghiniana, v. 26, p. 55–62.

Fauqué, L., Limarino, C., Cingolani, C., and Varela, R., 1999, Los movimientos intracarboniferos en la Precordillera riojana, *in* XIV° Congreso Geológico Argentino, Actas, v. 1, p. 421–424.

Fielding, C.R., Frank, T.D., Birgenheier, L.P., Rygel, M.C., Jones, A.T., and Roberts, J., 2008a, Stratigraphic imprint of the late Palaeozoic ice age in eastern Australia: A record of alternating glacial and nonglacial climate regime: Journal of the Geological Society of London, v. 165, p. 129–140.

Fielding, C.R., Frank, T.D., and Isbell, J.L., 2008b, The late Paleozoic ice age—A review of current understanding, *in* Fielding, C.R., Frank, T.D., and Isbell, J.L., eds., Resolving the Late Paleozoic Ice Age in Time and Space: Geological Society of America Special Paper 441, p. 41–57.

Frakes, L.A., Francis, J.E., and Syktus, J.I., 1992, Climate Modes of the Phanerozoic: Cambridge, UK, Cambridge University Press, 274 p.

Gastaldo, R.A., DiMichele, W.A., and Pfefferkorn, H.W., 1996, Out of the icehouse into the greenhouse: A late Paleozoic analogue for modern global vegetational change: GSA Today, v. 10, no. 10, p. 1–7.

Gerstenberger, H., and Haase, G., 1997, A highly effective emitter substance for mass spectrometric Pb isotope ratio determinations: Chemical Geology, v. 136, p. 309–312, doi: 10.1016/S0009-2541(96)00033-2.

González, C.R., 1981, Pavimento glaciario en el Carbonico de la Precordillera (Glacial pavement in the Carboniferous of the Precordillera): Revista de la Asociación Geológica Argentina, v. 36, p. 262–266.

González, C.R., 1990, Development of the late Paleozoic glaciations of the South American Gondwana in western Argentina: Palaeogeography, Palaeoclimatology, Palaeoecology, v. 79, p. 275–287, doi: 10.1016/0031-0182(90)90022-Y.

Gradstein, F.M., Ogg, J.G., Smith, A.G., Agterberg, F.P., Bleeker, W., Cooper, R.A., Davydov, V., Gibbard, P., Hinnov, L.A., House, M.R., Lourens, L., Luterbacher, H.-P., McArthur, J., Melchin, M.J., Robb, L.J., Sadler, P.M., Shergold, J., Villeneuve, M., Wardlaw, B.R., Ali, J., Brinkhuis, H., Hilgen, F.J., Hooker, J., Howarth, R.J., Knoll, A.H., Laskar, J., Monechi, S., Powell, J., Plumb, K.A., Raffi, I., Röhl, U., Sanfilippo, A., Schmitz, B., Shackleton, N.J., Shields, G.A., Strauss, H., Van Dam, J., Veizer, J., van Kolfschoten, Th., and Wilson, D., 2004, A Geologic Time Scale 2004: Cambridge, UK, Cambridge University Press, 610 p.

Gulbranson, E., Limarino, C.O., Marenssi, S., Montañez, I.P., Tabor, N.J., Davydov, V.I., and Colombi, C., 2008, Glacial deposits in the Rio Del Peñon Formatino, late Carboniferous, Rio Blanco Basin, northwestern Argentina: Latin American Journal for Sedimentology and Basin Analysis, v. 15, p. 129–142.

Gutiérrez, P.R., and Limarino, C.O., 2001, Palinología de la Formación Malanzán (Carbonifero Superior), La Rioja, Argentina: Nuevos datos y consideraciones paleoambientales: Ameghiniana, v. 38, p. 99–118.

Gutiérrez, P.R., and Limarino, C.O., 2006, El perfil del sinclinal del Rincón Blanco (noroeste de La Rioja): El límite Carbonífero-Pérmico en el noroeste Argentina: Ameghiniana, v. 43, p. 687–703.

Heckel, P.H., 1994, Evaluation of evidence for glacio-eustatic control over marine Pennsylvanian cyclothems in North America and consideration of possible tectonic effects, *in* Dennison, J.M., and Ettensohn, F.R., eds., Tectonic and Eustatic Controls on Sedimentary Cycles, Concepts in Sedimentology and Paleontology Volume 4: Tulsa, Oklahoma, SEPM (Society of Sedimentary Geology), p. 65–87.

Heckel, P.H., 2002, Overview of Pennsylvanian cyclothems in Midcontinent North America and brief summary of those elsewhere in the world, *in* Hills, L.V., Henderson, C.M., and Bamber, E.W., eds., Carboniferous and Permian of the World: Canadian Society of Petroleum Geologists Memoir 19, p. 79–98.

Heckel, P.H., 2008, Pennsylvanian cyclothems in Midcontinent North America as far-field effects of waxing and waning of Gondwana ice sheets, *in* Fielding, C.R., Frank, T.D., and Isbell, J.L., eds., Resolving the Late Paleozoic Ice Age in Time and Space: Geological Society of America Special Paper 441, p. 275–289.

Henry, L.C., Isbell, J.L., and Limarino, C.O., 2008, Carboniferous glacigenic deposits of the Protoprecordillera of west central Argentina, *in* Fielding, C.R., Frank, T.D., and Isbell, J.L., eds., Resolving the Late Paleozoic Ice Age in Time and Space: Geological Society of America Special Paper 441, p. 131–142.

Horbury, A.D., 1989, The relative roles of tectonism and eustasy in the deposition of the Urswick Limestone Formation in south Cumbria and north Lancashire, *in* Arthurton, R.S., Gutteridge, P., and Nolan, S.C., eds., The Role of Tectonics in Devonian and Carboniferous Sedimentation in the British Isles: Yorkshire Geological Society Occasional Publication 6, p. 153–169.

Isbell, J.L., Miller, M.F., Wolfe, K.L., and Lenaker, P.A., 2003, Timing of late Paleozoic glaciation in Gondwana: Was glaciation responsible for the development of Northern Hemisphere cyclothems?, *in* Chan, M.A., and Archer, A.A., eds., Sedimentary Giants—Extreme Depositional Environments: Geological Society of America Special Paper 370, p. 5–24.

Isbell, J.L., Cole, D.I., and Catuneanu, O., 2008a, Dwyka glaciation in the main Karoo Basin, South Africa: Stratigraphy, depositional controls, and glacial dynamics, *in* Fielding, C.R., Frank, T.D., and Isbell, J.L., eds., Resolving the Late Paleozoic Ice Age in Time and Space: Geological Society of America Special Paper 441, p. 71–82.

Isbell, J.L., Koch, Z.J., Szablewski, G.M., and Lenaker, P.A., 2008b, Permian glacigenic deposits in the Transantarctic Mountains, Antarctica, *in* Fielding, C.R., Frank, T.D., and Isbell, J.L., eds., Resolving the Late Paleozoic Ice Age in Time and Space: Geological Society of America Special Paper 441, p. 59–70.

Jenny, H., 1980, The Soil Resource: New York, Springer-Verlag, 377 p.

Jones, A.T., and Fielding, C.R., 2004, Sedimentological record of the late Paleozoic glaciation in Queensland, Australia: Geology, v. 32, p. 153–156, doi: 10.1130/G20112.1.

Kaczorek, D., Sommer, M., Andruschkewitsch, I., Oktaba, L., Czerwinski, Z., and Stahr, K., 2004, A comparative micromorphological and chemical study of "Raseneisenstein" (bog iron ore) and "Ortstein": Geoderma, v. 121, p. 83–94, doi: 10.1016/j.geoderma.2003.10.005.

Keller, M., 1999, Argentine Precordillera, *in* Basu, A., ed., Sedimentary and plate tectonic history of a Laurentian crustal fragment in South America: Geological Society of America Special Paper 341, p. 1–118.

Kneller, B., Milana, J.P., Buckee, C., and Al Ja'aidi, O.S., 2004, A depositional record of deglaciation in a paleofjord (late Carboniferous [Pennsylvanian] of San Juan Province, Argentina); the role of catastrophic sedimentation: Geological Society of America Bulletin, v. 116, p. 348–367, doi: 10.1130/B25242.1.

Krogh, T.E., 1973, A low contamination method for hydrothermal decomposition of zircon and extraction of U and Pb for isotopic age determinations: Geochimica et Cosmochimica Acta, v. 37, p. 485–494, doi: 10.1016/0016-7037(73)90213-5.

Limarino, C.O., and Spalletti, L.A., 1986, Eolian Permian deposits in west and northwest Argentina: Sedimentary Geology, v. 49, p. 109–127, doi: 10.1016/0037-0738(86)90017-5.

Limarino, C.O., and Spalletti, L.A., 2006, Paleogeography of the Upper Paleozoic basins of South America: An overview: Journal of South American Earth Sciences, v. 22, p. 134–155, doi: 10.1016/j.jsames.2006.09.011.

Limarino, C.O., Spalletti, L.A., and Siano, C., 1993, A Permian arid paleoclimatic phase in West and Northwest Argentina: Comptes Rendus, XII International Congress on the Carboniferous and Permian, Buenos Aires, v. 2, p. 453–468.

Limarino, C.O., Césari, S.N., Net, L.I., Marenssi, S.A., Gutiérrez, P.R., and Tripaldi, A., 2002, The Upper Carboniferous postglacial transgression in the Paganzo and Río Blanco Basins (northwestern Argentina): Facies and stratigraphic significance: Journal of South American Earth Sciences, v. 15, p. 445–460, doi: 10.1016/S0895-9811(02)00048-2.

Limarino, C., Tripaldi, A., Marenssi, S., and Fauqué, L., 2006, Tectonic, sea-level, and climatic controls on late Paleozoic sedimentation in the western basins of Argentina: Journal of South American Earth Sciences, v. 33, p. 205–226.

López Gamundí, O.R., 1987, Depositional models for the glacimarine sequences of Andean late Paleozoic basins of Argentina: Sedimentary Geology, v. 52, p. 109–126, doi: 10.1016/0037-0738(87)90018-2.

López Gamundí, O.R., 1997, Glacial-postglacial transition in the late Paleozoic basins of southern South America, *in* Martini, I.P., ed., Late Glacial and Postglacial Environmental Changes: Quaternary, Carboniferous-Permian, and Proterozoic: Oxford, UK, Oxford University Press, p. 147–168.

López-Gamundí, O.R., 2006, Permian plate margin volcanism and tuffs in adjacent basins of west Gondwana: Age constraints and common characteristics: Journal of South American Earth Sciences, v. 22, p. 227–238, doi: 10.1016/j.jsames.2006.09.012.

López-Gamundí, O.R., and Breitkreuz, 1997, Carboniferous to Triassic evolution of the Panthalassan margin in southern South America, *in* Dickins, J.M., Zuniy, Y., Hongfu, Y., Lucas, S.G., and Acharyya, S., eds., Late Paleozoic and Early Mesozoic Circum-Pacific Events and Their Global Correlation, World and Regional Series Volume 10: Cambridge, UK, Cambridge University Press, p. 8–19.

López-Gamundí, O.R., and Martinez, M., 2003, Esquema estratigrafico-secuencial para las unidades neopaleozoicas de la cuenca Calingasta-Uspallata en el flanco occidental de la Precordillera (Sequence stratigraphy of Upper Paleozoic units in the Calingasta-Uspallata Basin, western flank of Precordillera): Revista de la Asociación Geológica Argentina, v. 58, p. 367–382.

Mack, G.H., James, W.C., and Monger, H.C., 1993, Classification of paleosols: Geological Society of America Bulletin, v. 105, p. 129–136, doi: 10.1130/0016-7606(1993)105<0129:COP>2.3.CO;2.

Marenssi, S.A., Tripaldi, A., Limarino, C.O., and Caselli, A.T., 2005, Facies and architecture of a Carboniferous grounding-line system from the Guandacol Formation, Paganzo Basin, northwestern Argentina: Gondwana Research, v. 8, p. 187–202, doi: 10.1016/S1342-937X(05)71117-5.

Martin, J.R., Redfern, J., and Aitken, J.F., 2008, A regional overview of the late Paleozoic glaciation in Oman, *in* Fielding, C.R., Frank, T.D., and Isbell, J.L., eds., Resolving the Late Paleozoic Ice Age in Time and Space: Geological Society of America Special Paper 441, p.175–186.

Matsch, C.L., and Ojakangas, R.W., 1991, Comparisons in depositional style of "polar" and "temperate" glacial ice; late Paleozoic Whiteout Conglomerate (West Antarctica) and late Proterozoic Mineral Fork Formation (Utah), *in* Anderson, J.B., and Ashley, G.M., eds., Glacial Marine Sedimentation; Paleoclimatic Significance: Geological Society of America Special Paper 261, p. 191–206.

Mattinson, J.M., 2005, Zircon U-Pb chemical abrasion ("CA-TIMS") method: Combined annealing and multi-step partial dissolution analysis for improved precision and accuracy of zircon ages: Chemical Geology, v. 220, p. 47–66, doi: 10.1016/j.chemgeo.2005.03.011.

Menning, M., Alekseev, A.S., Chuvashov, B.I., Davydov, V.I., Devuyst, F.-X., Forke, H.C., Grunt, T.A., Hance, L., Heckel, P.H., Izokh, N.G., Jin, Y.-G., Jones, P.J., Kotlyar, G.V., Kozur, H.W., Nemyrovska, T.I., Schneider, J.W., Wang, X.-D., Weddige, K., Weyer, D., and Work, D.M., 2006, Global time scale and regional stratigraphic reference scales of Central and West Europe, East Europe, Tethys, South China, and North America as used in the Devonian-Carboniferous-Permian correlation chart 2003 (DCP 2003): Palaeogeography, Palaeoclimatology, Palaeoecology, v. 240, p. 318–372.

Miller, J.S., Matzel, J.E.P., Miller, C.F., Burgess, S.D., and Miller, R.B., 2007, Zircon growth and recycling during the assembly of large, composite arc plutons: Journal of Volcanology and Geothermal Research, v. 167, p. 282–299, doi: 10.1016/j.jvolgeores.2007.04.019.

Montañez, I.P., Tabor, N.J., DiMichele, W., Cecil, B., Eros, J.M., Gulbranson, E.L., and Poulsen, C., 2008, Paleotropical climate and vegetation linkages to southern Gondwana glaciation: Extending the Early Permian record into the late Mississippian: Geological Society of America Abstracts with Programs, v. 40, no. 6, p. 534.

Net, L.I., and Limarino, C.O., 2006, Applying sandstone petrofacies to unravel the Upper Carboniferous

evolution of the Paganzo Basin, northwest Argentina: Journal of South American Earth Sciences, v. 22, p. 239–254, doi: 10.1016/j.jsames.2006.09.010.

Net, L.I., Susana Alonso, M., and Limarino, C.O., 2002, Source rock and environmental control on clay mineral associations, lower section of Paganzo Group (Carboniferous): Northwest Argentina: Sedimentary Geology, v. 152, p. 183–199, doi: 10.1016/S0037-0738(02)00068-4.

Ogg, J.G., Ogg, G., and Gradstein, F.M., 2008, The Concise Geologic Time Scale: Cambridge, UK, Cambridge University Press, 177 p.

Pankhurst, R., Rapela, C., and Fanning, C.M., 2000, Age and origin of coeval TTG, I- and S-type granites in the Famatinian belt of NW Argentina: Transactions of the Royal Society of Edinburgh, Earth Sciences, v. 91, p. 151–168.

Parrish, J.T., 1993, Climate of the supercontinent Pangea: The Journal of Geology, v. 101, p. 215–233, doi: 10.1086/648217.

Parrish, R.R., Bowring, S.A., Condon, D.J., Schoene, B., Crowley, J.L., and Ramezani, J., 2006, EARTHTIME U-Pb tracer for community use: Goldschmidt Conference Abstracts, v. 76, p. A473, doi: 10.1016/j.gca.2006.06.1409.

Pazos, P.J., 2002a, Palaeoenvironmental framework of the glacial-postglacial transition (late Paleozoic) in the Paganzo-Calingasta Basin (southern South America) and the Great Karoo–Kalahari Basin (southern Africa): Ichnological implications: Gondwana Research, v. 5, p. 619–640, doi: 10.1016/S1342-937X(05)70634-1.

Pazos, P.J., 2002b, The late Carboniferous glacial to postglacial transition: Facies and sequence stratigraphy, western Paganzo Basin, Argentina: Gondwana Research, v. 5, p. 467–487, doi: 10.1016/S1342-937X(05)70736-X.

Perez Loinaze, V.S., 2007, A Mississippian miospore biozone for southern Gondwana: Palynology, v. 31, p. 101–118, doi: 10.2113/gspalynol.31.1.101.

Powell, R.D., 1991, Grounding-line systems as second-order controls on fluctuations of tidewater termini of temperate glaciers, *in* Anderson, J.B., and Ashley, G.M., eds., Glacial Marine Sedimentation; Paleoclimatic Significance: Geological Society of America Special Paper 261, p. 75–94.

Rabenhorst, M.C., and Swanson, D., 2000, Histosols, *in* Sumner, M.E., ed. Handbook of Soil Science: Boca Raton, Florida, CRC Press, p. E183–209.

Ramos, V.A., 2004, Cuyania, an exotic block to Gondwana: Review of a historical success and the present problems: Gondwana Research, v. 7, p. 1009–1026, doi: 10.1016/S1342-937X(05)71081-9.

Ramos, V.A., Jordan, T.E., Allmendinger, R.W., Kay, S.M., Cortes, J.M., and Palma, M.A., 1984, Chilenia; un terreno alóctono en la evolucion Paleozoica de los Andes centrales (Chilenia; an allochthonous terrain in the Paleozoic evolution of the Central Andes): Actas del Congreso Geológico Argentino, v. 2, p. 84–106.

Reid, M.R., and Coath, C.D., 2000, In situ U-Pb ages of zircons from the Bishop Tuff: No evidence for long crystal residence times: Geology, v. 28, p. 443–446, doi: 10.1130/0091-7613(2000)28<443:ISUAOZ>2.0.CO;2.

Remesal, M., Fauqué, L.A., and Limarino, C.O., 2004, Volcanismo calcoalcalino neopaleozoico en la Precordillera de La Rioja. Petrología y caracterización litoestratigráfica de la Formación Punta del Agua (Carbonífero Superior-Pérmico Inferior): Revista de la Asociación Geológica Argentina, v. 59, p. 462–476.

Rocha-Campos, A.C., dos Santos, P.R., and Canuto, J.R., 2008, Late Paleozoic glacial deposits of Brazil: Paraná Basin, *in* Fielding, C.R., Frank, T.D., and Isbell, J.L., eds., Resolving the Late Paleozoic Ice Age in Time and Space: Geological Society of America Special Paper 441, p. 97–114.

Rygel, M.C., Fielding, C.R., Frank, T.D., and Birgenheier, L.P., 2008, The magnitude of late Paleozoic glacioeustatic fluctuations: A synthesis: Journal of Sedimentary Research, v. 78, p. 500–511.

Scalabrini Ortiz, J., 1973, El Carbónico en el sector septentrional de la Precordillera sanjuanina: Revista de la Asociación Geológica Argentina, v. 27, no. 4, p. 351–377.

Schmitz, M.D., and Schoene, B., 2007, Derivation of isotope ratios, errors, and error correlations for U-Pb geochronology using ^{205}Pb-^{235}U-(^{233}U)-spiked isotope dilution thermal ionization mass spectromatic data: Geochemistry, Geophysics, Geosystems, v. 8, no. 8, doi: 10.1029/2006GC001492.

Scotese, C.R., and Barrett, S.F., 1990, Gondwana's movement over the South Pole during the Palaeozoic: Evidence from lithological indicators of climate, *in* McKerrow, W.S., and Scotese, C.R., eds., Palaeozoic Palaeogeography and Biogeography: Geological Society of London Memoir 12, p. 75–85.

Scotese, C.R., Boucot, A.J., and McKerrow, W.S., 1999, Gondwanan palaeogeography and palaeoclimatology: Journal of African Earth Sciences, v. 28, p. 99–114, doi: 10.1016/S0899-5362(98)00084-0.

Smith, L.B., and Read, J.F., 2000, Rapid onset of late Paleozoic glaciation on Gondwana: Evidence from Upper Mississippian strata of the midcontinent, United States: Geology, v. 28, p. 279–282, doi: 10.1130/0091-7613(2000)28<279:ROOLPG>2.0.CO;2.

Smith, L.B., and Read, J.F., 2001, Discrimination of local and global effects on Upper Mississippian stratigraphy, Illinois Basin, U.S.A.: Journal of Sedimentary Research, v. 71, p. 985–1002, doi: 10.1306/040501710985.

Southard, R.J., and Southard, A.R., 1985, Genesis of cambic and argillic horizons in two northern Utah Aridisols: Soil Science Society of America Journal, v. 49, p. 167–171.

Staff, S.S., 2006, Keys to Soil Taxonomy (10th ed.): Washington, DC, U.S. Department of Agriculture Natural Resources Conservation Service, 341 p.

Stewart, T.G., 1991, Glacial-marine sedimentation from tidewater glaciers in the Canadian High Arctic, *in* Anderson, J.B., and Ashley, G.M., eds., Glacial Marine Sedimentation; Paleoclimatic Significance: Geological Society of America Special Paper 261, p. 95–106.

Stollhofen, H., Werner, M., Stanistreet, I.G., and Armstrong, R.A., 2008, Single zircon U-Pb dating of Carboniferous-Permian tuffs, Namibia, and the intercontinental deglaciation cycle framework, *in* Fielding, C.R., Frank, T.D., and Isbell, J.L., eds., Resolving the Late Paleozoic Ice Age in Time and Space: Geological Society of America Special Paper 441, 83–96.

Streel, M., and Theron, J.N., 1999, The Devonian-Carboniferous boundary in South Africa and the age of the earliest episode of the Dwyka glaciation: New palynological result: Episodes, v. 22, p. 41–44.

Syvitski, J.P.M., 1989, On the deposition of sediment within glacier-influenced fjords: Oceanographic controls: Marine Geology, v. 85, p. 301–329, doi: 10.1016/0025-3227(89)90158-8.

Taboada, A.C., 1985, Estratigrafia y contnido paleontologico de la Formacion Agua del Jagüel, Permico Inferior de la Precordillera Mendocina: Primeras Jornadas Sobre Geologia de Precordillera, San Juan Acta I: San Juan, v. 1, p. 181–186.

Tabor, N.J., and Montañez, I.P., 2005, Oxygen and hydrogen isotope compositions of Permian pedogenic phyllosilicates: Development of modern surface domain arrays and implications for paleotemperature reconstructions: Palaeogeography, Palaeoclimatology, Palaeoecology, v. 223, p. 127–146, doi: 10.1016/j.palaeo.2005.04.009.

Thomas, G.S.P., and Connell, R.J., 1985, Iceberg drop, dump, and grounding structures from Pleistocene glacio-lacustrine sediments, Scotland: Journal of Sedimentary Petrology, v. 55, p. 243–249.

Thompson, R., and Mitchell, J.G., 1972, Palaeomagnetic and radiometric evidence for the age of the lower boundary of the Kiaman magnetic interval in South America: Geophysical Journal, v. 27, p. 207–214.

Torsvik, T.H., and Cocks, L.R.M., 2004, Earth geography from 400 to 250 Ma: A palaeomagnetic, faunal and facies review: Journal of the Geological Society of London, v. 161, p. 555–572, doi: 10.1144/0016-764903-098.

Van der Voo, R., and Torsvik, T.H., 2001, Evidence for late Paleozoic and Mesozoic non-dipole fields provides an explanation for the Pangea reconstruction problem: Earth and Planetary Science Letters, v. 187, p. 71–81, doi: 10.1016/S0012-821X(01)00285-0.

Veevers, J.J., and Powell, C.M., 1987, Late Paleozoic glacial episodes in Gondwanaland reflected in transgressive-regressive depositional sequences in Euramerica: Geological Society of America Bulletin, v. 98, p. 475–487, doi: 10.1130/0016-7606(1987)98<475:LPGEIG>2.0.CO;2.

Vepraskas, M.J., 1994, Redoximorphic Features for Identifying Aquic Conditions: North Carolina Agricultural Research Service Technical Bulletin, no. 301.

Visser, J.N.J., 1989, The Permo-Carboniferous Dwyka Formation of Southern Africa; deposition by a predominantly subpolar marine ice sheet: Palaeogeography, Palaeoclimatology, Palaeoecology, v. 70, p. 377–391, doi: 10.1016/0031-0182(89)90115-6.

Visser, J.N.J., 1991, The paleoclimatic setting of the late Paleozoic marine ice sheet in the Karoo Basin of southern Africa, *in* Anderson, J.B., and Ashley, G.M., eds., Glacial Marine Sedimentation; Paleoclimatic Significance: Geological Society of America Special Paper 261, 181–190.

Wendt, I., and Carl, C., 1991, The statistical distribution of the mean squared weighted deviation: Chemical Geology, v. 86, p. 275–285.

Wright, V.P., and Tucker, M.E., 1991, Calcretes: An Introduction: Oxford, UK, International Association of Sedimentologists, Blackwell Scientific, 352 p.

Wright, V.P., and Vanstone, S.D., 2001, Onset of late Paleozoic glacio-eustasy and the evolving climates of low latitude areas: A synthesis of current understanding: Geological Society of London Journal, v. 158, p. 579–582.

York, D., 1967, The best isochron: Earth and Planetary Science Letters, v. 2, p. 479–482, doi: 10.1016/0012-821X(67)90193-8.

York, D., 1969, Least squares fitting of a straight line with correlated errors: Earth and Planetary Science Letters, v. 5, p. 320–324, doi: 10.1016/S0012-821X(68)80059-7.

Zempolich, W.G., Cook, H.E., Zhemchuzhnikov, V.G., Zorin, A.Y., Giovannelli, A., Viaggi, M., Lehmann, P.J., Fretwell, N., Zhaimina, V.Y., Buvtyshkin, V.M., and Alexeiev, D.V., 2002, Biotic and abiotic influence on the stratigraphic architecture and diagenesis of middle to late Paleozoic carbonates of the Bolshon Karatau Mountains, Kazakhstan and the southern Urals, Russia: Implications for the distributions of early marine cements and reservoir quality in subsurface reservoirs, *in* Zempolich, W.G., and Cook, H.E., eds., Paleozoic Carbonates of the Commonwealth of Independent States (CIS): Subsurface Reservoirs and Outcrop Analogs: Society for Sedimentary Geology (SEPM) Special Publication 74, p. 123–180.

Manuscript Received 3 February 2009
Revised Manuscript Received 11 September 2009
Manuscript Accepted 19 September 2009

Printed in the USA